SECURITY CLASSIFICATION OF THIS PAGE

REPORT DOCUMENTATION PAGE

1a. REPORT SECURITY CLASSIFICATION: Unclassified	1b. RESTRICTIVE MARKINGS
2a. SECURITY CLASSIFICATION AUTHORITY	3. DISTRIBUTION / AVAILABILITY OF REPORT: As required to Defense Documentation Center individuals and organizations on ONR program
2b. DECLASSIFICATION / DOWNGRADING SCHEDULE	
4. PERFORMING ORGANIZATION REPORT NUMBER(S): Final Report	5. MONITORING ORGANIZATION REPORT NUMBER(S): N-00014-83-C0141
6a. NAME OF PERFORMING ORGANIZATION: Honeywell Ceramics Center; 6b. OFFICE SYMBOL (If applicable)	7a. NAME OF MONITORING ORGANIZATION
6c. ADDRESS (City, State, and ZIP Code): 5121 Winnetka Avenue North, New Hope, MN 55428	7b. ADDRESS (City, State, and ZIP Code)
8a. NAME OF FUNDING / SPONSORING ORGANIZATION: Office of Naval Research; 8b. OFFICE SYMBOL (If applicable)	9. PROCUREMENT INSTRUMENT IDENTIFICATION NUMBER
8c. ADDRESS (City, State, and ZIP Code): Division of Materials Research, 800 N. Quincy, Arlington, VA 22217	10. SOURCE OF FUNDING NUMBERS: PROGRAM ELEMENT NO. / PROJECT NO. / TASK NO. / WORK UNIT ACCESSION NO.

11. TITLE (Include Security Classification): Mechanical Reliability of Piezoelectric and Dielectric Ceramics

12. PERSONAL AUTHOR(S): K. D. McHenry and B.G. Koepke

13a. TYPE OF REPORT	13b. TIME COVERED	14. DATE OF REPORT (Year, Month, Day)	15. PAGE COUNT
Final	FROM 6/1/83 TO 6/1/87	6/1/88	

16. SUPPLEMENTARY NOTATION

17. COSATI CODES			18. SUBJECT TERMS (Continue on reverse if necessary and identify by block number)
FIELD	GROUP	SUB-GROUP	Crack propagation, fracture toughness, multilayer dielectrics

19. ABSTRACT (Continue on reverse if necessary and identify by block number)

Mechanical Reliability of various piezoelectric and dielectric ceramic materials has been investigated with respect to material anisotropy and operational environments. A variety of fracture mechanics testing techniques have been employed to characterize subcritical crack growth in multilayer PZT and multilayer Z5U capacitors. Subcritical crack growth is extremely sensitive to environment (chemical and electrical) as well as geometrical anisotropy of the multilayer structures.

20. DISTRIBUTION / AVAILABILITY OF ABSTRACT: ☐ UNCLASSIFIED/UNLIMITED ☐ SAME AS RPT ☐ DTIC USERS	21. ABSTRACT SECURITY CLASSIFICATION: Unclassified
22a. NAME OF RESPONSIBLE INDIVIDUAL	22b. TELEPHONE (Include Area Code) / 22c. OFFICE SYMBOL

DD FORM 1473, 84 MAR — 83 APR edition may be used until exhausted. All other editions are obsolete.

SECURITY CLASSIFICATION OF THIS PAGE

Mechanical Reliability of Piezoelectric and Dielectric Ceramics

Table of Contents

J

pulte

A-1

SECTION 1

K. D. McHenry and B. G. Koepke. Electric Field Effects on Subcritical Crack Growth in PZT. Honeywell Ceramics Center, New Hope, MN, 1983.

ELECTRIC FIELD EFFECTS ON SUBCRITICAL CRACK GROWTH IN PZT

K.D. McHenry and B.G. Koepke[+]
Honeywell Ceramics Center
New Hope, Minnesota 55428

[+] Honeywell Systems and Research Center
Minneapolis, Minnesota 55440

ABSTRACT

Subcritical crack growth in the transducer ceramic, PZT has been studied utilizing the double torsion testing geometry in dead-weight loading. The effects of applied electric fields on crack progagation were studied in both poled and unpoled material. High a.c. and d.c. fields applied perpendicular to the crack front enhanced crack propagation in unpoled PZT. The frequency of the applied a.c. field did not measurably effect the crack propagation except at mechnical resonance frequencies. In poled PZT, the application of an a.c. or d.c. field perpendicular to the crack plane always "turned" the crack in a direction opposite to the poling direction. These results can be rationalized in terms of a mixed mode fracture originating in the anisotropic electromechanical response of the material.

INTRODUCTION

Subcritical crack growth in PZT can be detrimental to the long term mechanical integrity of the material and also to the electrical characteristics of the device. For example, flaws in the material may act as sources of corona discharge which contribute to electrical noise.

The phenomenon of subcritical crack growth has been studied extensively in many ceramic materials but has only recently been investigated in piezoelectric ceramics. Freiman et al. [1] have shown that water enhances slow crack growth in a Navy Type I PZT, and Caldwell and Bradt [2] have studied slow crack growth in PZT using dynamic fatigue tests. Bruce et al. [3] have shown that water enhances subcritical crack growth in a Navy Type III high drive sonar PZT and that the kinetics of crack growth could be described by a thermally activated process. In addition, crack growth characteristics in poled material were different depending upon the poling direction.

The effects of applied electric fields on subcritical crack growth in ceramic materials is not well understood and has only been investigated for a few materials. Bhaduri and Wang [4] have shown that low level applied d.c. fields enhance slow crack growth in single-crystal silicon.

Caso and Frechette [5] found that d.c. fields applied perpendicular to a propagating crack retard or stop crack propagation in glass. The situation in PZT and probably other piezoelectrics is more complicated due to the nature of the piezoelectric effect.

The two phenomena that play a role when an electric field is applied to a material are electrostriction and the piezoelectric effect. Both phenomena respond to an electric field by inducing shape changes to the material. The piezoelectric effect in general provides greater dimensional changes and is present only in piezoelectric materials. Piezoelectric materials not only change shape with the application of an electric field but also exhibit the converse effect (i.e., the generation of charge upon the application of a mechanical stress).

In this paper we present the results of an extensive series of measurements in which slow crack growth in PZT was examined as a function of applied field. Both a.c. and d.c. fields were applied to poled and unpoled PZT.

EXPERIMENTAL PROCEDURE

Test Technique

Subcritical crack growth in PZT was studied using the double torsion technique popularized by Evans et al., [6, 7]. A schematic showing the specimen and loading geometry is shown in Figure 1. The stress intensity for this configuration is independent of the crack length and is given by

$$K_I = PW_m\left[\frac{3(1+\nu)}{Wd^3 d_n}\right]^{1/2} = AP \qquad (1)$$

where P is the load, ν is Poisson's ratio and the other terms are identified in Figure 1.

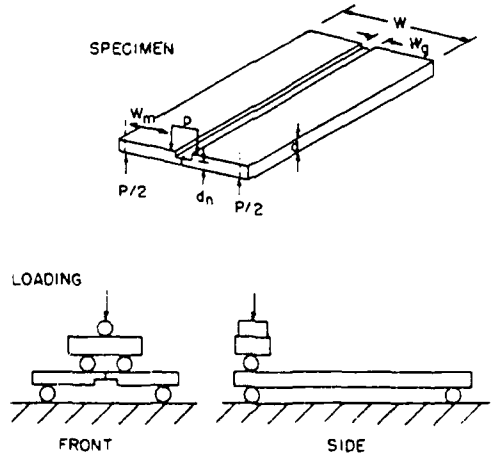

Figure 1. Schematic Showing Specimen and Loading Geometry For Double Torsion Tests

The dead weight loading technique was used to obtain slow crack growth results. In this technique, a fixed load is applied to a precracked double torsion specimen. Crack growth is then measured by monitoring the deflection of the specimen versus time with an LVDT. The crack velocity is then obtained by

$$V = \frac{1}{BP} \frac{dv}{dt} \qquad (2)$$

where B is the slope of the compliance curve (i.e., specimen deflection vs. applied load), P is the applied load, and dy/dt is the measured deflection rate. Unlike the load relaxation technique where a complete (K_I[-V) curve can be theoretically obtained from one relaxation test, the dead weight loading technique yields one data point per test. To obtain other points. the dead weight load is either increased or decreased and the correspoi ding change in deflection rate is measured.

The dead weight loading technique has proven to be the only viable technique for obtaining slow crack growth measurements in PZT subject to the application of electric fields. In a load relaxation test when the PZT specimen is under fixed grip conditions and an electric field is applied to the specimen, the piezoelectric effect causes the specimen to change dimensions such that erroneous loading conditions are generated. The dead weight loading technique corrects this problem by providing a fixed load regardless of dimensional changes in the specimen. It should also be pointed out that the electrostrictive effect generated in all materials subjected to an electric field will give rise to the same phenomena of dimensional change. Depending upon the magnitude of the electrostrictive effect in the material in question, similar erroneous results could be obtained with the load relaxation technique.

The samples were PZT plates nominally 2.54 cm (1 inch) wide, 7.62 cm (3 inches) long and had a thickness ranging from 17 mm (.070) to 20 mm (.080 inch). A side groove was cut in each specimen to a depth of about one-half the specimen thickness and to a width of approximately 3mm [8]. Before testing, the specimens were precracked in an Instron TM testing machine at a crosshead speed of 5×10^{-3} mm/min. The specimens were then placed in the dead weight loading test apparatus and loads sufficient to cause crack propagation were applied. Once crack growth was observed, an electric field was applied to the specimen, and the change in deflection rate was measured. The duration of each particular test ranged from 30 seconds to 2 minutes depending upon the crack velocity. Longer times were used for slower crack velocities to insure accurate determinations of deflection rates.

Material and Testing Environments

The PZT specimens tested in this study were cut from transducer tubes manufactured by the Honeywell Ceramics Center. The PZT is a Navy Type III high drive sonar ceramic with a nominal composition of $Pb_{0.94}$ $Sr_{0.06}$ $Ti_{0.47}$ $Zr_{0.53}$ O_3 plus proprietary additions. This composition is tetragonal below the Curie point and is dielectrically "hard". The tubes

were manufactured by cold isostatic pressing and sintering. All samples were cut from unpoled tubes with a 100 grit diamond cut-off wheel and subsequently surface ground to shape with a 100 grit diamond wheel. All grinding was done wet.

The specimens were tested while submersed in a mineral oil in order to suppress corona discharge during the application of the electric fields. In all cases the electric fields were applied perpendiuclar to the crack plane. Bruce et al.[3] found that poling parallel to the crack plane played no significant role in crack propagation in PZT. Thus all tests in this study were conducted with the applied fields perpendicular to the crack plane. The fields were applied via an electrode configuration shown in Figure 2. The electrodes are shown as shaded areas and consisted of a conductive paint containing silver. These electrodes were then covered by an insulating varnish.

Poled Specimens

Composite double torsion specimens as shown in Figure 3 were fabricated to study the effects of electric fields on crack propagation in poled PZT. The specimen was produced by first poling a 5 mm wide PZT beam and then cementing it between two wider unpoled PZT beams with high strength conducting epoxy. A side groove was then machined in the poled section and the surfaces trued before testing. The electrodes were painted on the specimen over the composite joints similar to those in Figure 2.

A narrow center section was required when testing poled specimens because the electrode spacing must be small to achieve the high fields required to pole the material. A field of 35 KV/cm was applied at 150°C for 2.5 minutes to pole the center section. The compliances of composite specimens were experimentally determined to be identical to that of an upoled specimen.

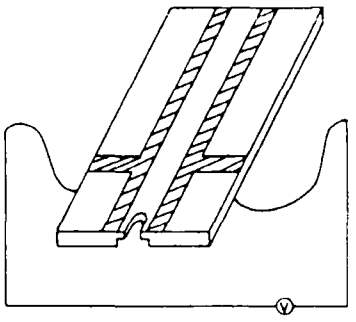

Figure 2. Schematic Showing Electrode Configuration Used To Apply Electric Fields To Double Torsion Specimens

RESULTS

Effects of a.c. and d.c. Fields on Unpoled PZT

The effects of a.c. fields applied perpendicular to the crack plane on crack propagation in unpoled PZT are shown in Figure 4. In this Figure the crack velocity is plotted as a function of the stress intensity factor. Each of the data points represents one dead weight loading measurement. Some data points have been omitted for clarity. The data have been fit by a least-squares linear regression analysis and the slopes are indicated on the Figure.

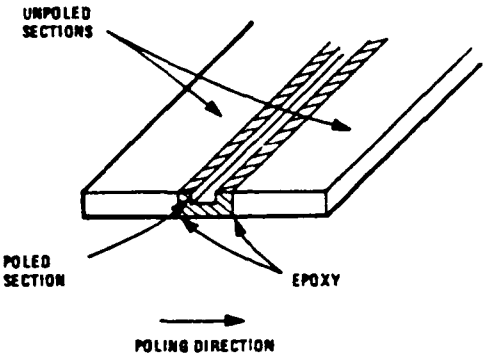

Figure 3. Schematic Showing Composite PZT Double Torsion Specimen With Poled Center Section Cemented Between Two Unpoled Sections

The voltages indicated on the Figure represent applied voltages over a spacing of approximately one-half centimeter (the electrode spacing). As a result, the applied field in a specimen is twice the indicated voltage (500 volts -> 1 KV/cm). All a.c. fields shown in Figure 4 were applied at a frequency of 2 KHz.

The baseline crack propagation data with a slope of n = 45 was obtained with the material submersed in distilled water. This data is in good agreement with that obtained by Bruce et al. [3] and by itself represents a fairly "corrosive" environment for PZT in comparison with moisture free environments such as mineral oil or Freon.

As mentioned previously, all crack propagation measurements with an applied electric field were conducted while the specimen was submersed in mineral oil to suppress corona discharge and to eliminate the effects of moisture on crack propagation. The overall effect of a.c. fields applied perpendicular to the crack plane in unpoled PZT is to enhance crack growth as shown in Figure 4. The (V - K_I) curves are shifted to lower values of stress intensity and become more shallow in slope indicating an enhnaced susceptibility to slow crack growth with increasing applied field strengths.

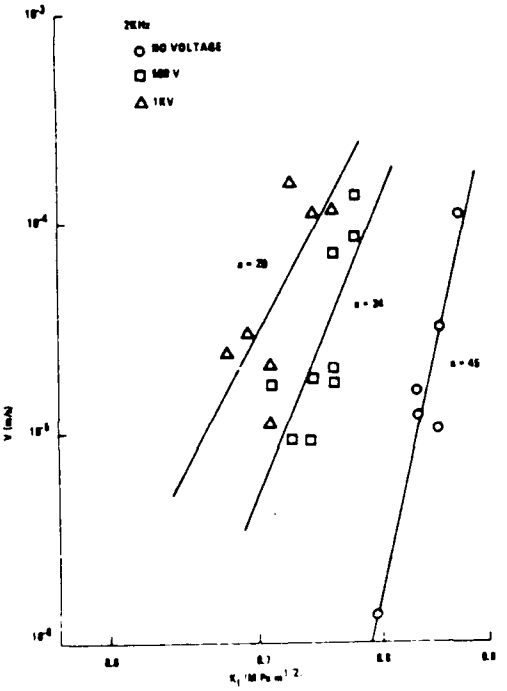

Figure 4. Effect of Applied a.c. Field Strength On Crack Propagation In Unpoled PZT

The effects of applied d.c. fields on crack propagation in unpoled PZT are represented in Figure 5. In this Figure, the straight line regression analyses from Figure 4 (a.c. fields) are plotted for comparsion. The individual data points have been omitted. Each regression analysis represents a minimum of 25 data points. The stress intensity axis in Figure 5 has been expanded making the slopes appear shallower than in Figure 4. As in Figure 4, the voltages represent applied voltages and must be multiplied by two to obtain field strengths.

A comparsion of the data indicates that applied d.c. fields have much the same effect as a.c. fields in enhancing crack propagation in unpoled PZT. Increasing applied d.c. fields enhance slow crack growth. The functional dependencies of decreasing slopes with increasing applied field strengths are nearly identical with regard to a.c. and d.c. fields. The major differences are that the velocities under d.c. applied fields are lower and the (V-K_I) curves intersect the (V-K_I) curve with no field applied. It should be noted also that the validity of the 4 KV d.c. data (8 KV/cm) remains in question. At this applied field it was observed that the crack deviated from its original plane in a direction against the applied d.c. field. As a result questions are raised as to whether the stress analysis commonly used for the double torsion specimen can be applied in this case. This point will be discussed in more detail in the next section.

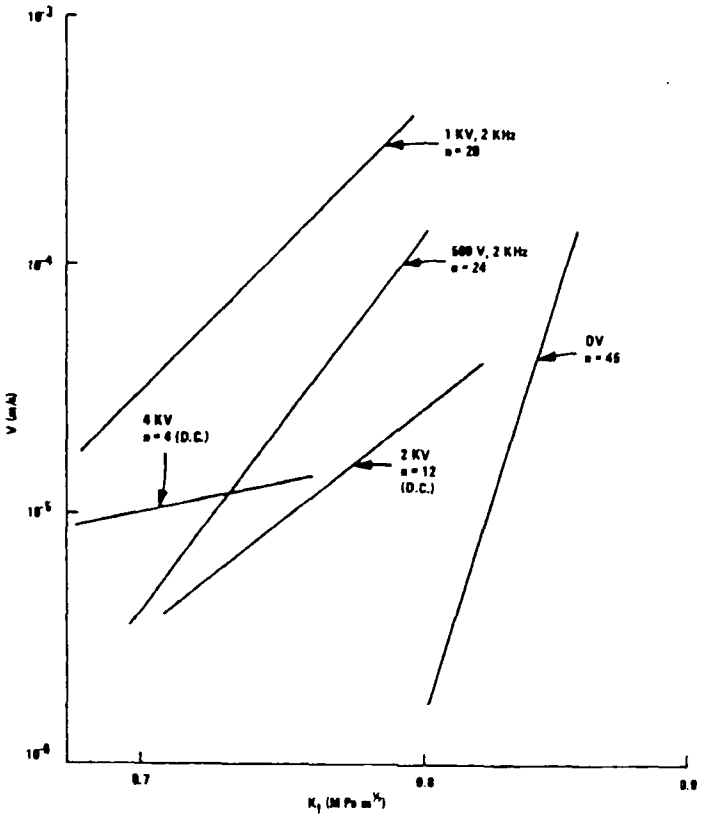

Figure 5. Effect of a.c. and d.c. Fields on Crack Propagation in Unpoled PZT

Clearly, there is some difference in the effect of a.c. versus d.c. fields on crack propagation in unpoled PZT as evidenced in Figure 5. One obvious difference of course, is that an a.c. field has a frequency associated with it. In Figure 6 we show a series of measurements where the frequency of the applied a.c. field (1 KV/cm) was varied to study its effects on slow crack growth. Surprisingly, within the scatter of the data, there is no apparent effect of the frequency of applied a.c. field on crack propagation in unpoled PZT. The enhancement of crack propagation (n = 18) over the baseline condition (n = 45) can be attributed solely to the applied field strength. The lack of a frequency dependence implies the absence of a hysteretic heating effect at the crack tip due to the applied field. Such an argument, therefore, is not valid in describing the enhanced crack velocities one observes with a.c. fields applied to PZT.

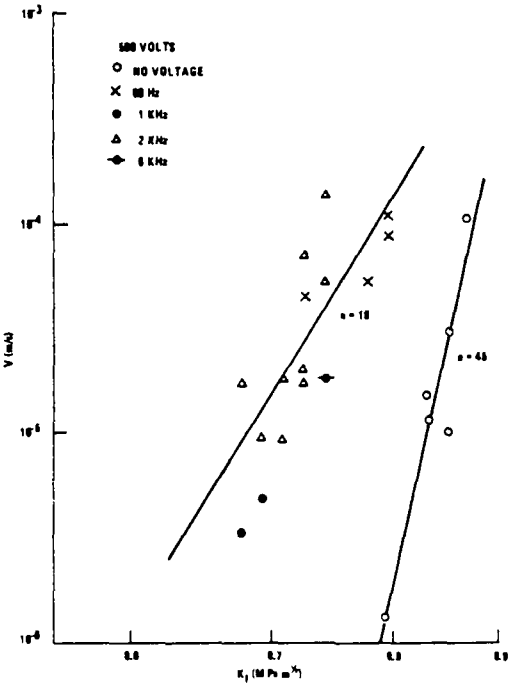

Figure 6. Effect of Frequency of Applied a.c. Field on Crack Propagation in Unpoled PZT.

There is also a mechanical resonance aspect to slow crack growth that must be considered when discussing the frequencies of applied a.c. fields. In Figure 7 the phenomenon of mechanical resonance is illustrated. Figure 7 represents a deflection vs. time trace of an actual experiment in which crack growth was generated in a specimen by the application of a 2.26 Kg load and a 1.4 KV/cm, 10 KHz a.c. field. A rapid increase in crack velocity was observed when the frequency was changed to 2.632 KHz. The crack velocity returned to the starting velocity when the frequency was changed to 1 KHz. At a frequency of 2.703 KHz, catastrophic failure ensued. The mechanical resonance frequency is crack length dependent and increases with increasing crack length in a double torsion specimen.

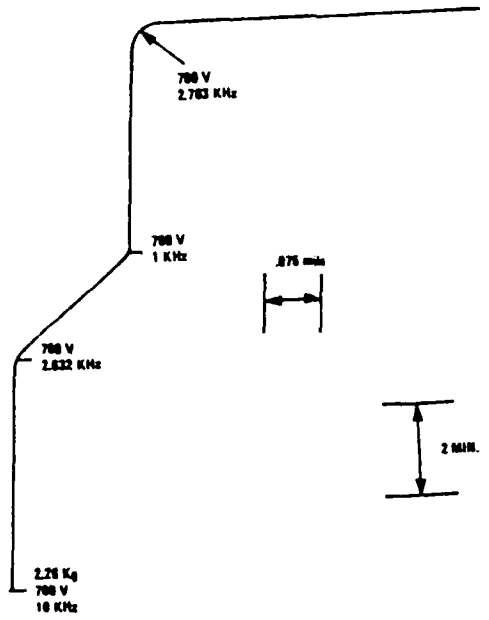

Figure 7. Deflection-Time Trace Indicating A Mechanical Resonance - Frequency of Applied a.c. Field Interaction on Slow Crack Growth in Unpoled PZT.

Effects of a.c. and d.c. Fields on Poled PZT

The effect of a.c. and d.c. fields applied perpendicular to the crack plane on crack propagation in poled PZT is shown in Figures 8 and 9. In all cases the crack deviated from its original plane and propagated in a direction against the poling direction in the material. This phenomena occurred regardless of a.c. field strength and frequency and d.c. field strength or direction of applied d.c. field (with and against the poling direction). Figure 8 clearly shows the deviation of the crack in a direction against the poling direction. Figure 9 shows that the applied fields also alter the crack front profile in the poled material. The fracture surface shown in Figure 9 was obtained by lightly tapping the specimen before and after the application of an electric field to demarcate crack profiles. This macroscopic evidence of a change in fracture behaviors would seem to indicate a mixed mode failure or the introduction of shear components to the stress distribution in the poled material. As noted in a previous section, this phenomena also occurs in unpoled material with the application of very high field strengths (> 8 KV/cm). Microstructurally, there appeared to be no difference in the fracture surface under all conditions studied in this work. Fracture was virtually 100% transgranular.

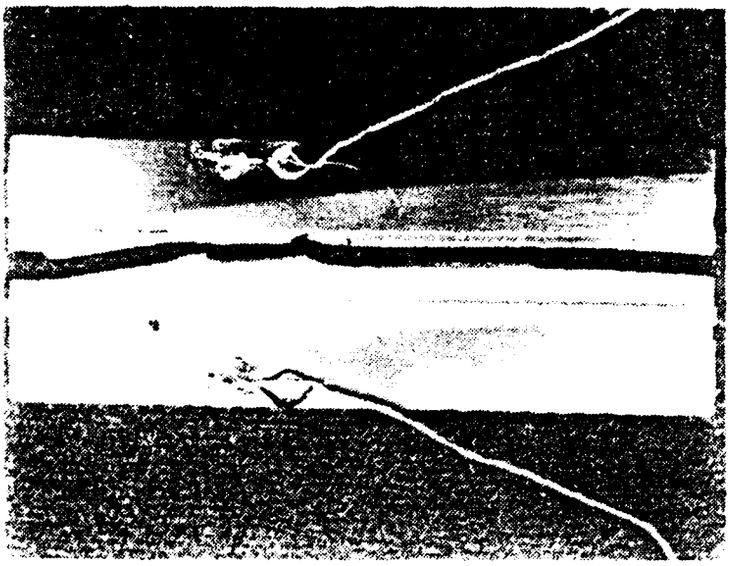

Figure 8. Deviation of Crack Propagation in a Direction A.ainst the Poling Direction in Poled PZT

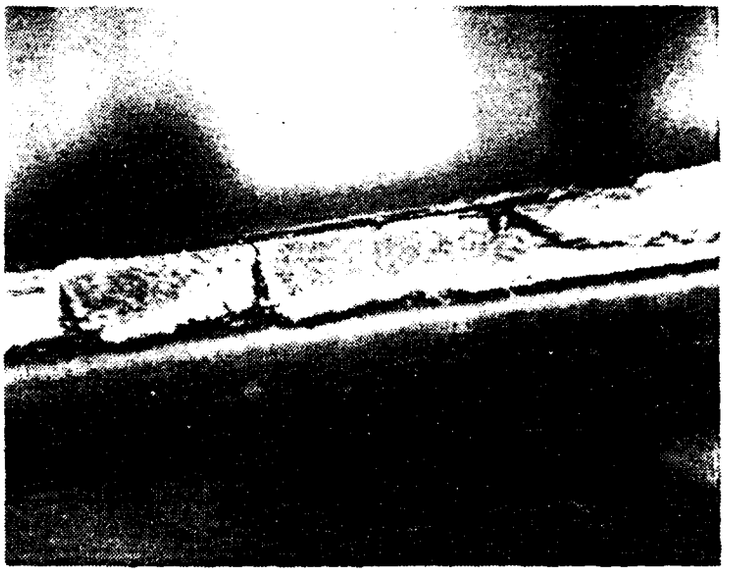

Figure 9. Change in the Crack F: nt Profile With Applied Electric Field in Poled PZT

DISCUSSION

The origin of a physical displacement or strain (ϵ) in a material in response to the application of an electric field (E) is given by

$$\epsilon_{jk} = d_{ijk}E_i + \gamma_{iljk}E_iE_l \qquad (3)$$

The first term to the right of the equality represents the piezoelectric effect and the second term represents the electrostrictive effect where d_{ijk} and γ_{iljk} are the piezoelectric and electrostrictive coefficients respectively. All materials exhibit an electrostrictive effect to some degree and it can be shown that this phenomena is responsible for retardation of slow crack growth in glass subjected to an electric field [9, 10]. The predominant effect in PZT is piezoelectric as a result of the very large piezoelectric coefficients encountered in this material.

Deeg [11] has performed a theoretical analysis which shows that crack growth in piezoelectrics may be arrested, slowed down or accelerated depending upon the applied stress, the applied field strength and a variety of material parameters and boundary conditions. This analysis and its applicability to the present results are beyond the scope of this paper and are to be treated in a separate work [12]. The major finding of this analysis is that shear stresses and mixed mode loading are generated at the crack tip as a result of the anisotropic piezoelectric nature of the material. We postulate that the shear stresses and resultant mixed mode loading are responsible for crack acceleration in unpoled PZT and crack deflection in poled PZT when subjected to applied electric fields. Only the background and origin of the phenomena will be described here.

Polycrystalline PZT in the unpoled state is isotropic. After poling the material has 4 mm symmetry. The piezoelectric coefficient matrix is given by [13]

$$\begin{pmatrix} 0 & 0 & 0 & 0 & d_{15} & 0 \\ 0 & 0 & 0 & d_{24} & 0 & 0 \\ d_{31} & d_{32} & d_{33} & 0 & 0 & 0 \end{pmatrix} \qquad (4)$$

and $d_{15} = d_{24}$,

$d_{31} = d_{31}$.

Typical values for the piezoelectric coefficients of a PZT Type III material are

$$d_{15} = 335 \times 10^{-12} \text{ m/V}$$
$$d_{31} = -96 \times 10^{-12} \text{ m/V} \qquad (5)$$
$$d_{33} = 215 \times 10^{-12} \text{ m/V}$$

The strains developed in a piezoelectric material by the application of an electric field are related to the piezoelectric coefficients and the field components by [14]

$$S_1 = d_{31} E_3,$$

$$S_2 = d_{31} E_3,$$

$$S_3 = d_{33} E_3, \qquad (6)$$

$$S_4 = d_{15} E_2,$$

$$S_5 = d_{15} E_1.$$

Thus the largest piezoelectric coefficient, d_{15}, is responsible for the generation of the shear strains S_4 and S_5.

The origin of the orthogonal components of the electric field (i.e., E_1 and E_2) in Equation 6 are schematically shown in Figure 10. This schematic is intended to represent a two-dimensional planar surface of a double torsion specimen subject to the application of an electric field in the three-direction. The thickness of the double torsion specimen would be in the one-direction. The effect of a crack in a dielectric such as PZT is to cause curvature of the field lines and a field intensification at the crack tip as shown in the Figure. While not shown here, similar effects are expected in the 1-2 plane as a result of the curved crack front profile normally encountered in the double torsion specimen. The exact curvature of the field lines and the field intensification at the crack tip are functions of the dielectric constants of the material and the media in the crack, the applied field strength and the radius of curvature of the crack tip.

Figure 10 demonstrates the origin of the E_2 components of the applied electric field as a result of the curvature of the field around the crack tip. A similar phenomena in the one-direction give rise to an E_1 component. Shear stresses are then developed according to Equation 6. We postulate that these shear stresses are responsible for crack deflection in poled PZT.

In unpoled PZT, which is originally isotropic, the effect of an applied electric field is to tend to pole the material and develop anisotropy. Even small applied fields resulted in some domain orientation and anisotropic piezoelectric effects. The shear strains that are developed, however, with small fields are not sufficient to cause the crack to deviate from its original plane but presumably interact in such a fashion as to cause mixed mode loading and crack acceleration. At an applied field strength of 8 KV/cm in unpoled PZT sufficient polarization has occurred in the material that the crack begins to deviate similar to the observation in the poled PZT.

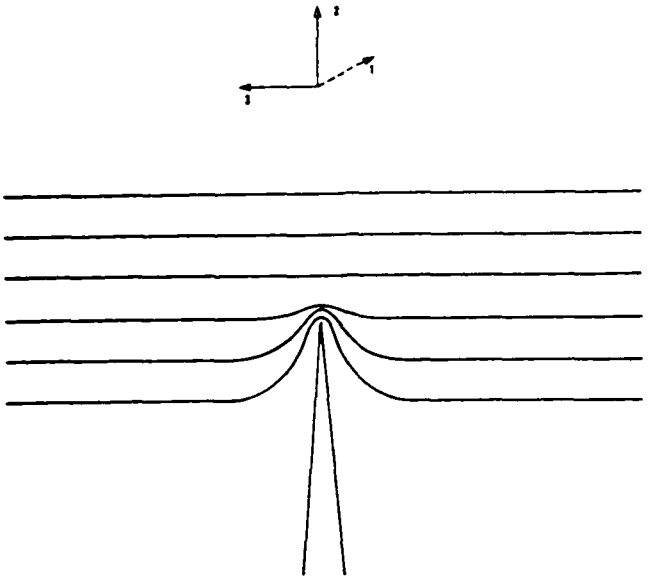

Figure 10. Contour of Field Lines in a Dielectric Material Due to the Presence of a Crack

ACKNOWLEDGEMENTS

The authors would like to express their gratitude to the Office of Naval Research for support of this effort under contract No. N0014-76-C-0625. The continued interest of Dr. R.C. Pohanka is gratefully acknowledged.

REFERENCES

1. S.W. Freiman, K.R. McKinney and H.L. Smith, in Fracture Mechanics of Ceramics, Vol. 2, R.C. Bradt, D.P.H. Hasselman and F.F. Lange, ed., Plenum Publishing Co., New York, NY (1974) p. 659.

2. R.F. Caldwell and R.C. Bradt, J. Amer. Ceram. Soc., 60, 169 (1977).

3. J.G. Bruce, W.W. Gerberich and B.G. Koepke, in Fracture Mechanics of Ceramics, Vol. 4, R.C. Bradt, D.P.H. Hasselman and F.F. Lange, ed., Plenum Publishing Co., New York, NY (1978) p. 687.

4. S. Bhaduri and F.F.Y. Wang, Bull. Amer. Ceram. Soc., 59, 826 (1980) Abstract Only.

5. G.B. Caso and V.D. Frechette, Bull. Amer. Ceram. Soc., 58, 342 (1979) Abstract Only.

6. A.G. Evans, J. Mater. Sci. 7, 1137 (1972).

7. D.P. Williams and A.G. Evans, J. Testing and Eval., 1, 264 (1973).

8. B.J. Pletka, E.R. Fuller, Jr. and B.G. Koepke, in Fracture Mechanics Applied to Brittle Materials, ASTM STP 678, S. Freiman, ed. Amer. Soc. for Testing and Materials, Philadelphia, PA (1979) p. 19.

9. T.E. Smith, Jr., "Stress Concentrations in Three-Dimensional Electrostriction," Ph.D. Thesis, University of Illinois (1966).

10. S.D. Brown, University of Illinois, Private Communication (1981).

11. W.F.J. Deeg, "Analysis of Dislocation, Crack, and Inclusion Problems in Piezoelectric Solids", Ph.D. Thesis, Stanford University (1980).

12. K.D. McHenry and B.G. Koepke, to be published.

13. J.F. Nye, Physical Properties of Crystals, Oxford (1976).

14. B. Jaffe, W.R. Cook, Jr. and H. Jaffe, Piezoelectric Ceramics, Academic Press, London (1971).

SECTION 2

K. D. McHenry and B. G. Koepke. Crack Propagation in Z5U Multilayer Dielectrics. Honeywell Ceramics Center, 5121 Winnetka Avenue North, New Hope, MN, 1984.

ABSTRACT

This technical report summarizes the progress made during the period June 1, 1983 - May 31, 1984 under Contract N00014-83-C0141 entitled ELECTROMECHANICAL INTEGRITY OF MULTILAYER DIELECTRIC AND PIEZOELECTRIC CERAMICS for the Office of Naval Research. During the first phase of the program, emphasis has been placed on the characterization of slow crack growth and fracture toughness of Z5U multilayer capacitor bodies as a function of environment (both chemical and electrical) and orientation of the multilayer structure.

It has been found that moisture has a deleterious effect in enhancing slow crack growth in Z5U multilayer ceramics similar to the effect shown in other ceramic materials. The enhancement of slow crack growth in the presence of moisture has been demonstrated for both parallel and perpendicular orientations of the multilayer structure with respect to the propagating crack. The application of DC electric fields to the multilayer ceramics either has no effect or serves to retard crack propagation depending upon the crack orientation with respect to the applied electric field.

The fracture toughness or critical stress intensity factor as measured by the double torsion testing technique has been found to vary with respect to orientation of the multilayer structure. Higher fracture toughness values are obtained when the macroscopic crack is forced to propagate in a direction perpendicular to the multilayer structure.

CRACK PROPAGATION IN Z5U MULTILAYER DIELECTRICS

I. INTRODUCTION

The use of multilayer ceramics in critical systems such as those used for navigation, guidance or surveillance has steadily been increasing over the past several years as multilayer technology has been extended to various ceramic materials. Multilayer $BaTiO_3$ based capacitors and alumina chip carriers have found wide spread usage in military as well as commercial applications. The multilayer technology has recently been applied to PZT materials, specifically for Naval applications, with the anticipated benefits including reduced drive voltages. In all of these applications, reliability of the actual component is of prime consideration. A great deal of effort has been expended on the development and implementation of reliable proof tests for sorting out faulty elements. Most capacitor elements produced today are 100% proof-tested. The basis of these proof tests is usually some electrical parameter of the element such as insulation resistance or capacitance. These type of tests are effective in screening out severely defective elements but may not eliminate components with very small flaws.

The basic structure of a monolithic ceramic body is schematically shown in Figure 1.[1] The individual layers may be anywhere from 25 to 125 microns (0.001 to 0.005") thick for multilayer capacitors up to over 600 microns (0.025") thick for multilayer monolithic PZT bodies. The individual layers are usually punched out of sheets of tape cast material, electroded, laminated and cofired as a single body. A variety of processing and/or production related defects may become apparent in such a structure. These defects are schematically shown in Figure 2[1] and include:

1. Void in dielectric material between opposed electrodes
2. Void in dielectric material outside of active electrode structure.
3. Crack between opposed electrodes
4. Crack from electrode to outside surface
5. Delamination of adjacent layers
6. Delimination from an electrode to opposite termination
7. End margin too short
8. Excessive variation of dielectric thickness
9. Inadequately bonded end metallization
10. Poorly attached lead
11. Improper stacking
12. Improper registration
13. Inadequate side margin

In applications where multilayer ceramic components are subjected to mechanical stress, any or all of the defects listed above may have a deleterious effect on the long term reliability of the component due to subcritical flaw growth. This flaw growth may actually lead to premature failure of the component either by catastrophic failure or electrical breakdown. Flaw growth in bulk dielectric and piezoelectric materials has been studied for some time [2, 3]. Much less work has been performed in determining subcritical crack growth characteristics of multilayer ceramic materials[4, 5].

In this report, we summarize the first year's effort of a program established to determine the fracture characteristics and anelastic deformation behavior of multilayer barium titanate capacitor materials and multilayer monolithic PZT materials. The bulk of the work performed in the first year has concentrated on the fracture behavior of multilayer capacitor materials.

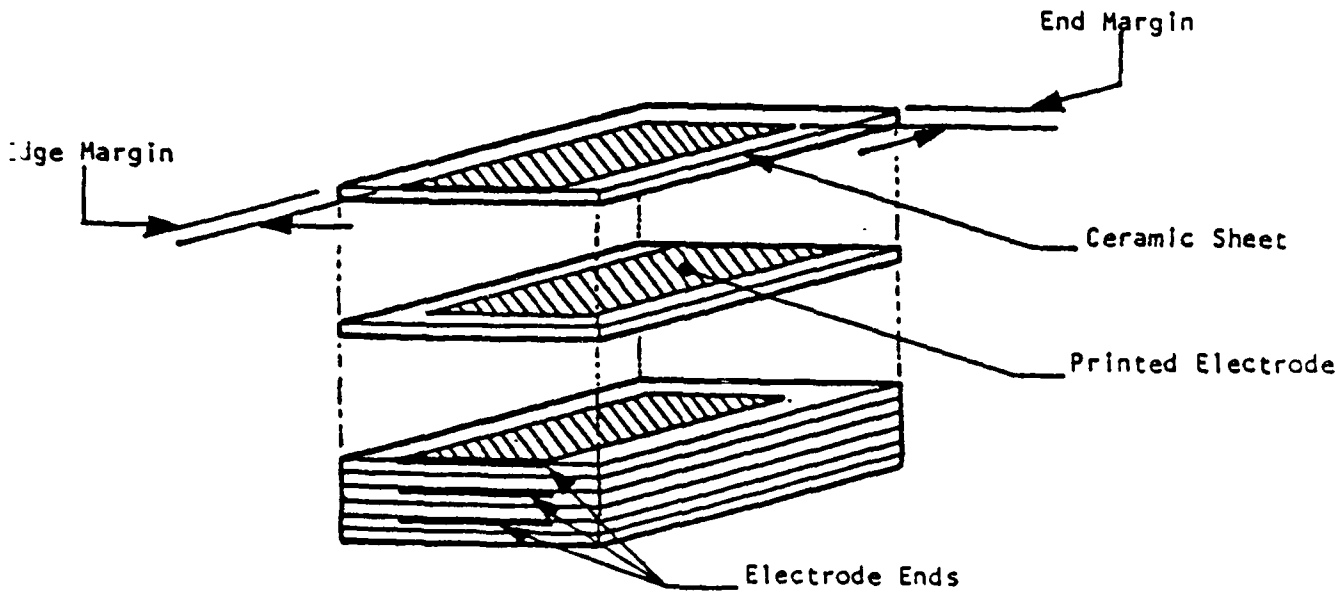

FIGURE 1: MONOLITHIC CAPACITOR STACKING ARRANGEMENT

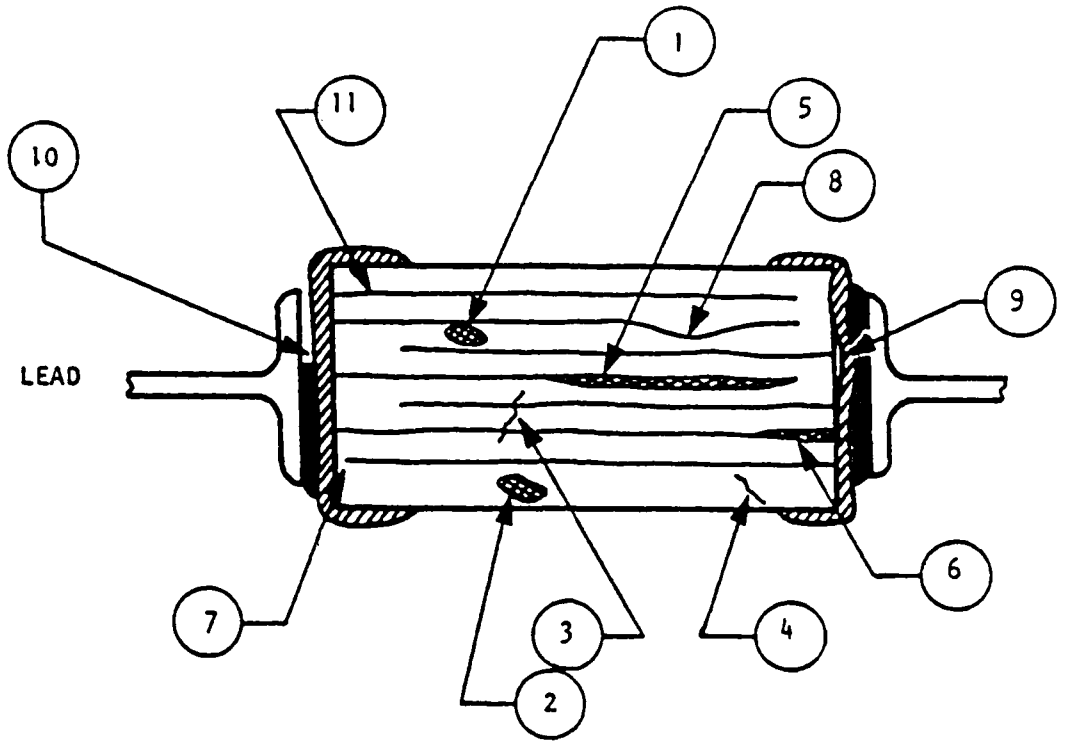

LONGITUDINAL SECTION

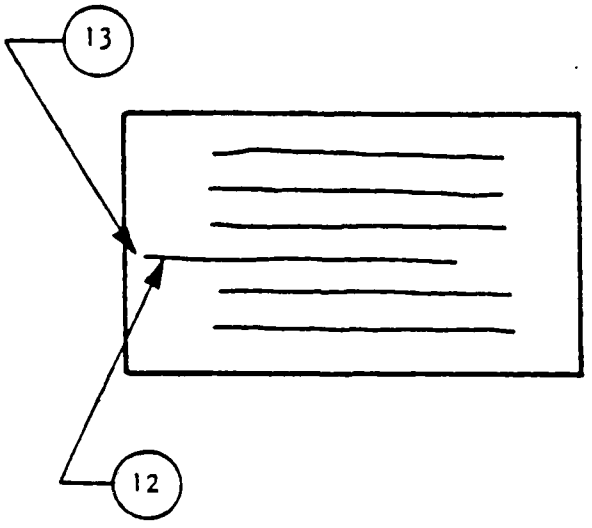

TRANSVERSE SECTION

FIGURE 2: CROSS-SECTIONED CAPACITORS ARRANGEMENT

II. EXPERIMENTAL PROCEDURE

A. SUBCRITICAL CRACK GROWTH TESTING

Subcritical crack growth in the multilayer capacitor material was studied using the double torsion (DT) technique popularized by Evans et al.[6, 7]. A schematic illustrating the specimen and loading geometry is shown in Figure 3. For this geometry, the stress intensity is independent of crack length over a majority of the specimen length and is given as

$$K_I = PW_m[3(1+v)/Wd^3d_n]^{1/2} \quad (1)$$

where P is the applied load, v is Poisson's ratio of the material, and the other terms are defined in Figure 3. The slow crack growth was obtained using the the dead-weight loading technique which the authors have used in past work on bulk PZT materials [8]. In this particular testing technique, a precracked specimen is subjected to a fixed applied load P less than the critical load necessary to cause catastrophic failure, P_{IC}. The deflection of the specimen is monitored by a Daytronic LVDT. If subcritical crack growth occurs, a linear increase in deflection is observed with time for a given crack velocity. Providing the compliance of the specimen is a linear function of crack length, it can be shown that the crack velocity is related to the fixed applied load and the rate of deflection according to (7).

$$V = (1/BP)\,(dy/dt) \quad (2)$$

where B is the slope of the compliance curve (specimen deflection vs applied load at various crack lengths), P, is the applied load and dy/dt is the measured deflection rate. Unlike the load relaxation testing technique where a complete (K_I-V) curve can be theoretically obtained from one relaxation test, the dead weight loading technique yields one data point per test. To obtain other points, the applied load must either be increased or decreased and the corresponding change in deflection rate measured.

The specimens used in the tests were plates measuring 2.4 cm (0.95") long, 1.8 cm (0.7") wide and 0.9-1.0 cm (0.035-0.040") in thickness. It was found early in the program that side grooves were unnecessary in assuring that the crack ran down the center of the specimen. In a few cases the crack would propagate out of the center line and these data were discarded.

In a typical test, a specimen was loaded at a very low deflection rate (typically 0.005 cm/min) in an Instron Testing Machine until a crack was initiated, indicated either by a rapid decrease in load or a leveling of the load. The specimen was then unloaded and transferred to the dead weight loading fixture for subcritical crack growth measurements. Depending on the applied load and the resultant crack velocity obtained, anywhere from 3 to 10 individual (K_I-V) data points could be collected from each specimen.

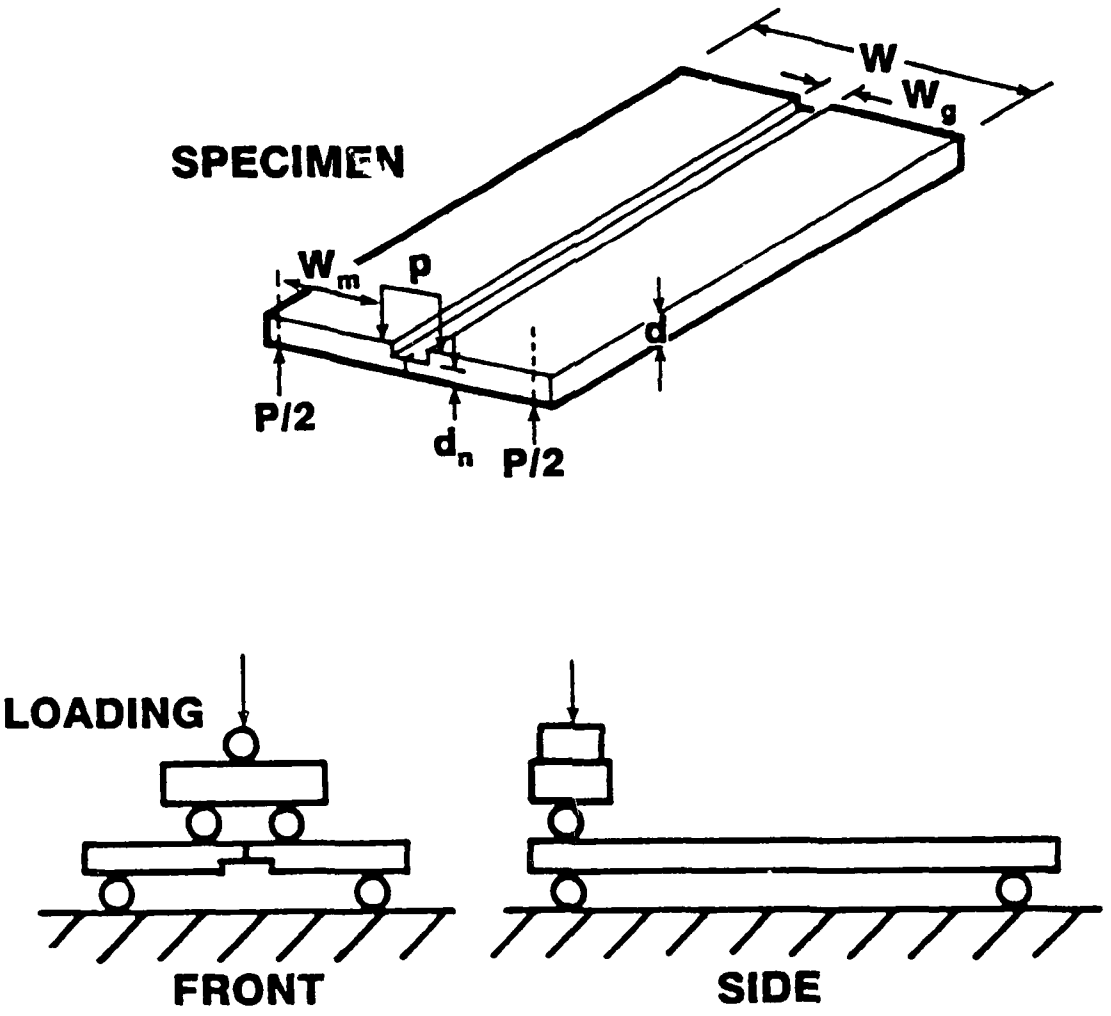

FIGURE 3: SCHEMATIC DOUBLE TORSION SPECIMEN AND LOADING GEOMETRY

B. FRACTURE TOUGHNESS TESTING

The fracture toughness or critical stress intensity factor, K_{IC}, was measured under rapid loading conditions in the Instron Testing Machine. A precracked specimen was loaded to failure at a deflection rate of 0.125 cm/min. The load at failure or critical load at fracture, P_{IC}, was used in Equation 1 to calculate K_{IC}.

C. MATERIAL AND TESTING ENVIRONMENTS

The barium titanate multilayer capacitor bodies used in the study were a standard Z5U composition supplied by Sprague Electric. The specimens were quite a bit oversized compared to normal capacitors and exhibited some degree of warpage in the as-received state. Some surface grinding had to be performed to achieve adequately flat and parallel specimens. The specimens as-received contained 7-8 individual electroded layers.

Samples were tested in a variety of environments selected for varying moisture content as well as in various electrical environments. Specimens were tested in ambient conditions (25°C and 45% R.H.), submersed in water and submersed in toluene. Electrical environments consisted primarily of applied d.c. fields of various field strengths. The application of electric fields was accomplished by painting stripes of conducting paint on the specimens and attaching leads.

D. COMPOSITE SPECIMEN FABRICATION

The macrostructure of multilayer ceramic bodies such as the ones considered in this investigation is highly anisotropic. As such, the electrical and mechanical properties are usually anisotropic. As shown in Figure 4, there are two crack orientations with respect to the macrostructure that must be considered. The situation where the crack front is perpendicular to the multilayer structure (the crack cuts across the layers) represents the normal testing that was performed on the as-received plates. In order to achieve the other orientation, it was necessary to fabricate composite specimens. This was accomplished by cutting a section from the edge of the specimen or from the middle of the specimen. The width of this section was approximately equal to the thickness of the overall specimen. The section was rotated 90° and epoxied back in as the central web. This provided the necessary configuration for propagating a crack parallel to the layers. The procedure for precracking the specimen, the method of slow crack growth evaluation and the procedure for measuring the fracture toughness were identical to those discussed previously.

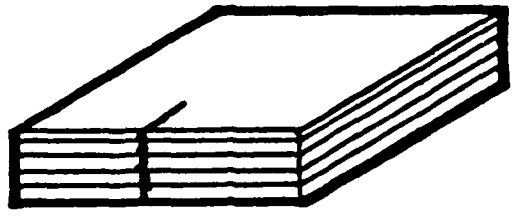

PERPENDICULAR ORIENTATION

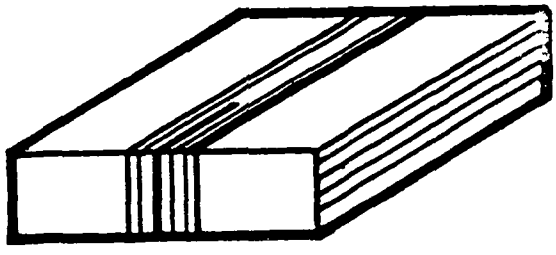

PARALLEL ORIENTATION

FIGURE 4: CRACK ORIENTATIONS WITH RESPECT TO MULTILAYER ORIENTATION

III. RESULTS AND DISCUSSION

A. COMPLIANCE MEASUREMENTS

Since the elastic analysis of a DT specimen is based upon the condition that the compliance of the specimen is a linear function of crack length, the compliances of a number of regular and composite specimens were measured as a function of crack length by artificially introducing cracks of known length with a very thin diamond blade. The results are shown in Figure 5. Due to the fact that the specimens had varying thicknesses as a result of grinding them flat, the results shown in Figure 5 are normalized by the thickness cubed, t^3, from the theoretical compliance of a DT specimen [7]. The slope of the data shown in Figure 5 was used to calculate the crack velocity according to Equation 2.

It's interesting to note that the compliances shown for the two differently constructed specimens in Figure 5 are equal. The silver-filled epoxy used in this investigation is the same type used previously in fracture studies of bulk PZT[3]. In that study, it was found that the compliances of regular specimens and composite specimens were virtually identical. The data shown in Figure 5 indicate that the compliances of the two different types of specimens are nearly equal and there appears to be no anisotropic microstructural effects.

Preliminary compliance measurements have been performed on multilayer monolithic PZT bodies and a different type of phenomenon has been observed. The PZT bodies are originally fabricated large enough such that DT specimens of both orientations can be obtained without having to fabricate composite specimens. In this case, indications are that the specimens are more compliant when the layered structure is parallel to the thickness of the specimen.

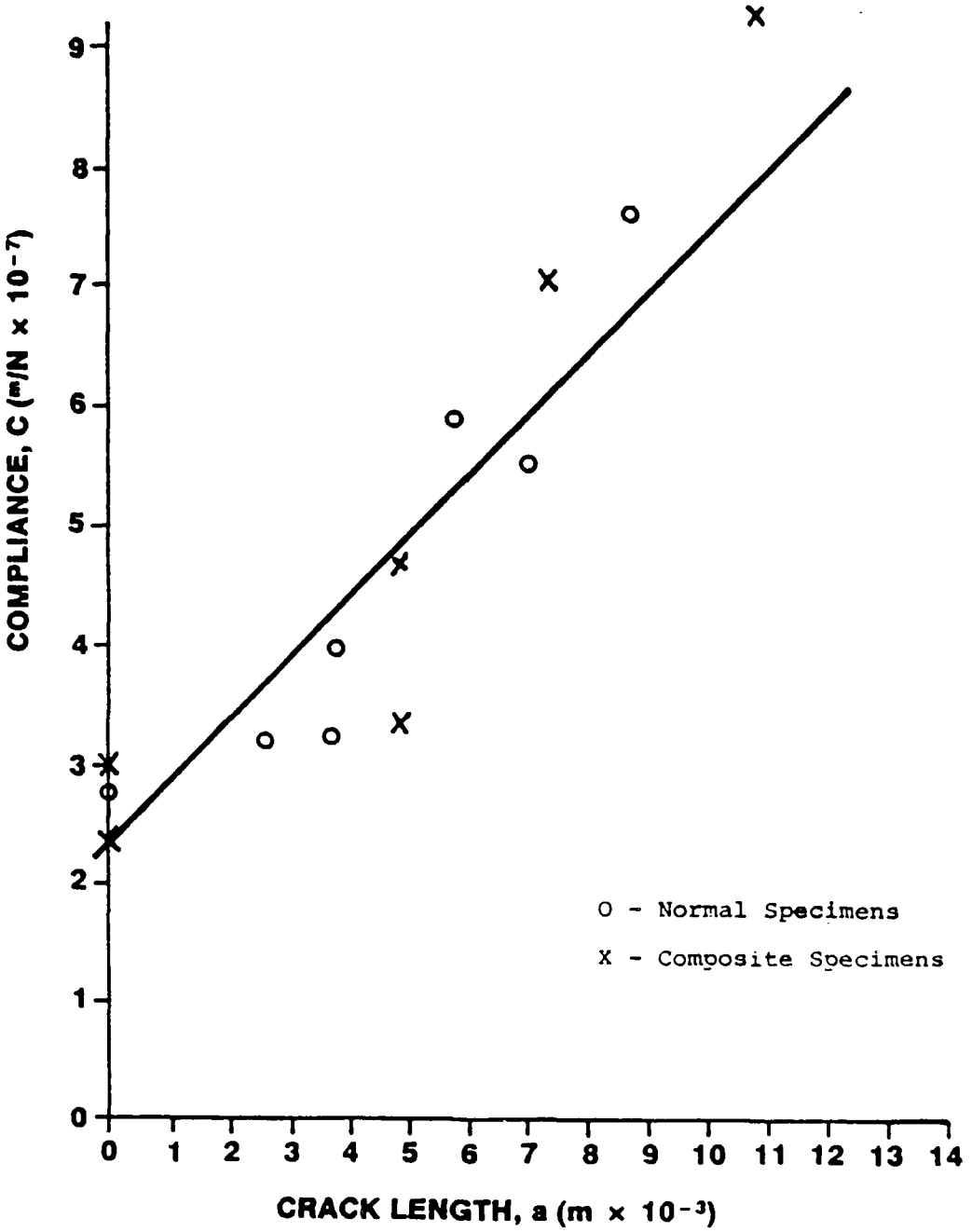

FIGURE 5: COMPLIANCE MEASUREMENTS OF Z5U MULTILAYER DIELECTRICS

B. SUBCRITICAL CRACK GROWTH

1. Environmental Effects

Slow crack growth results for Z5U specimens tested in the perpendicular orientation (regular specimens where crack front is perpendicular to the layers) in media containing various amounts of water are shown in Figure 6. Environmental effects on slow crack growth in composite specimens will be discussed under Orientation Effects. The figure is plotted as the logarithm of the crack velocity versus the logarithm of the applied stress intensity factor. With the data plotted in this fashion, the slope, n, is a measure of the stress corrosion susceptibility of the material. A low value of n which is the case for the data taken in a water environment indicates a greater susceptibility to stress corrosion. For the sake of clarity some of the individual data points have been deleted from Figure 6. The reproducibility of the individual data points collected from a single specimen as well as sample to sample reproducibility was outstanding. Such reproducibility can either be a result of very homogeneous material or an averaging effect since the crack front at any given time is intersecting 7-8 layers of material. In the other orientation discussed later, a marked lack of reproducibility is observed.

The overall significance of the data shown in Figure 6 is that like most other ceramic materials this multilayer capacitor material is very susceptible to moisture enhanced slow crack growth. The data taken in a toluene environment with a slope in excess of 100 is probably indicative of Stage III crack propagation while the other data are probably representative of Stage I crack propagation or stress corrosion. The susceptibility of this material to moisture enhanced slow crack growth is similar in nature and magnitude to that observed in BX and NPO type capacitor materials [5]. Unlike the case of crack propagation in BX and NPO types of capacitors, no evidence of Stage II crack growth was observed indicating that this Z5U material has a sensitivity to moisture enhanced crack propagation over a wider range of applied stress and crack velocity before transport of water to the crack tip becomes rate limiting.

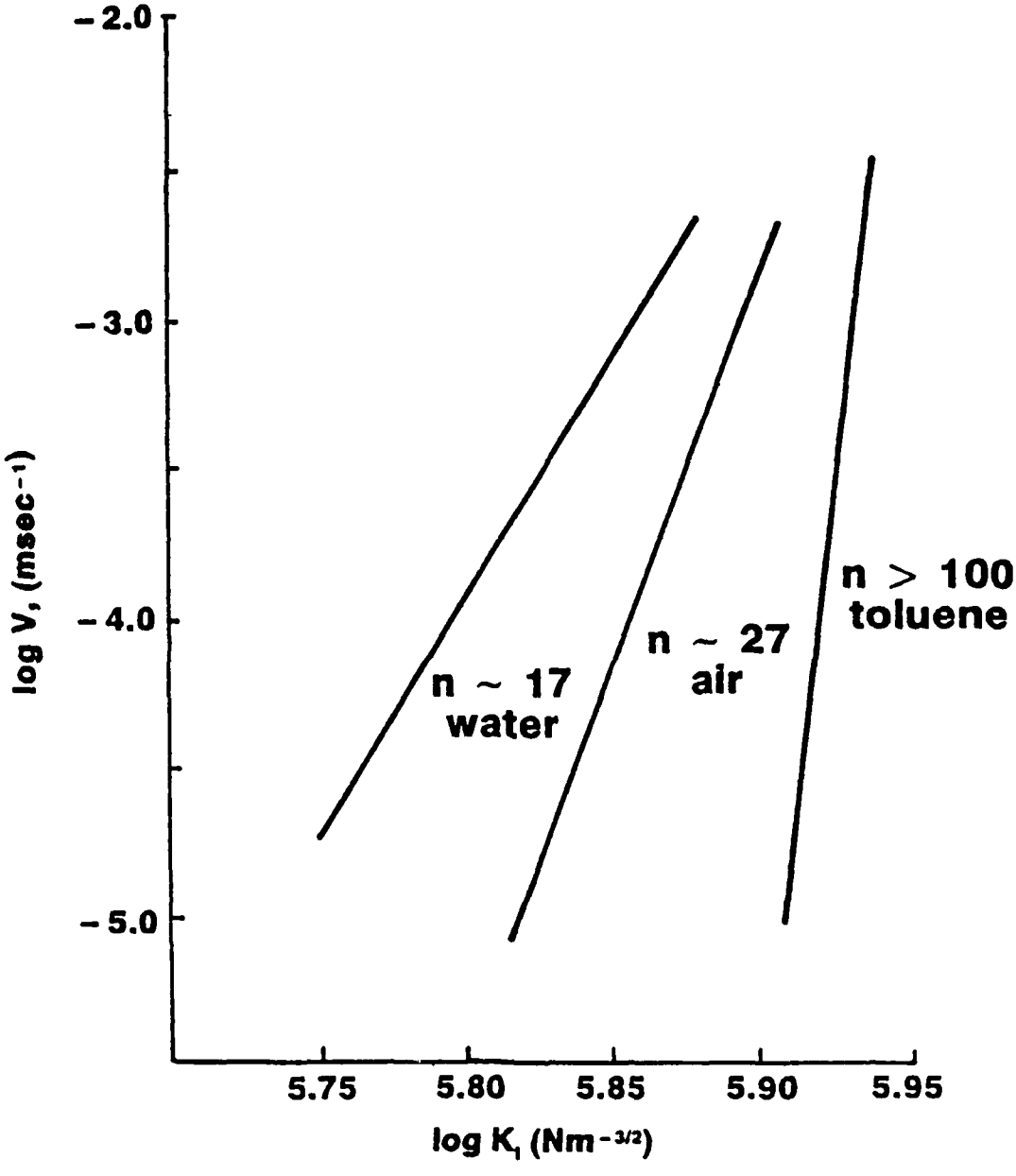

FIGURE 6: EFFECT OF MOISTURE ON SUBCRITICAL CRACK GROWTH IN PERPENDICULAR ORIENTATION

2. Electrical Effects

The effect of the application of a d.c. field to a multilayer specimen on the crack propagation is schematically shown in Figure 7. The figure is an actual deflection vs time trace obtained during a dead weight loading experiment. In this particular case, the applied load yielded a stress intensity of 8×10^5 $Nm^{-3/2}$ and a crack velocity of 1×10^{-5} m/sec. All electrical tests were performed with the specimens submersed in Flourinert to prevent discharge. This represents a relatively moisture free environment and as such the crack velocity and stress intensity correspond well with data taken in a toluene environment.

The important thing to notice is that for this orientation no increase or decrease in crack velocity is seen with the application of a d.c. field. In this orientation the crack front is perpendicular to the layered structure and the application of a voltage to the specimen results in an electric field being established parallel to the propagating crack tip. It is not anticipated that a field parallel to the crack should significantly interact with and alter the propagation of that crack. This same type of behavior has been observed in other multilayer capacitor materials [5] as well as in bulk PZT [3, 8]. In the case of bulk PZT, no alteration of crack propagation was observed in either poled or unpoled material when the electrical field was parallel to the propagating crack or the polarization direction was parallel to the propagating crack.

3. Orientation Effects

Up to the point all the results have been presented in terms of one specimen orientation, namely, that where the crack propagation is perpendicular to the layered structure of the capacitor specimens. The other orientation is that for which the composite specimens were fabricated. Quite different behavior is noted in this orientation.

In Figure 8 data are shown for tests conducted on parallel oriented specimens in an ambient environment. Unlike crack growth in the other orientation, the data shown in Figure 8 exhibit a tremendous amount of scatter. In general, most of the data do indeed lie at lower applied stress intensity factors than the data for the perpendicular orientation in ambient. However, the great deal of scatter prohibits the use of regression analysis to provide a meaningful interpretation of the data.

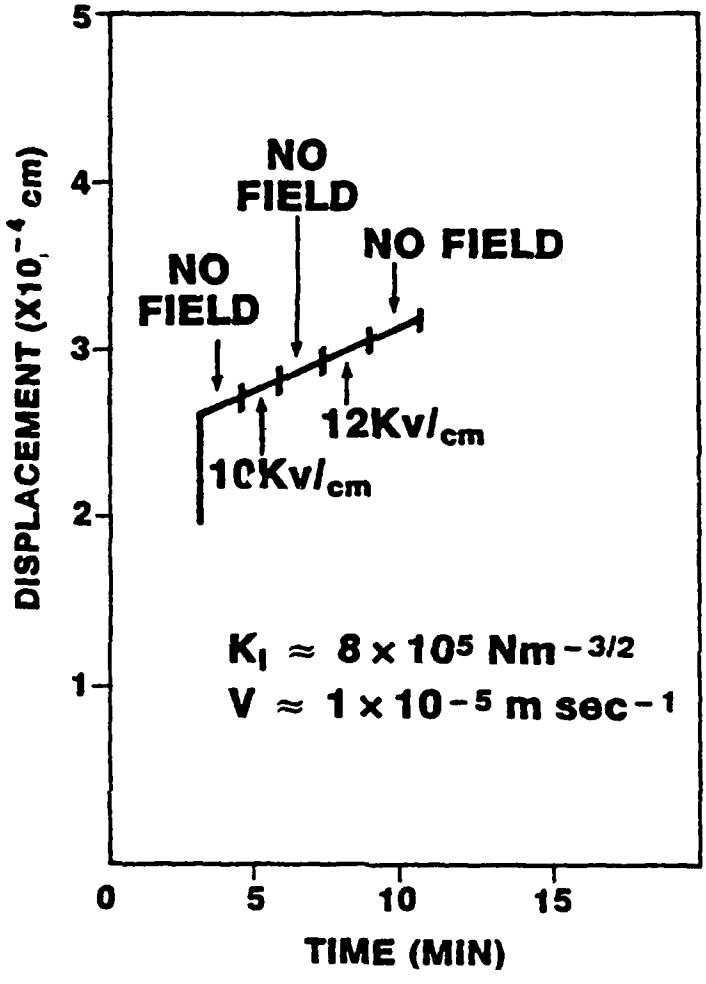

FIGURE 7: EFFECT OF DC FIELD ON SLOW CRACK GROWTH IN PARALLEL DIRECTION

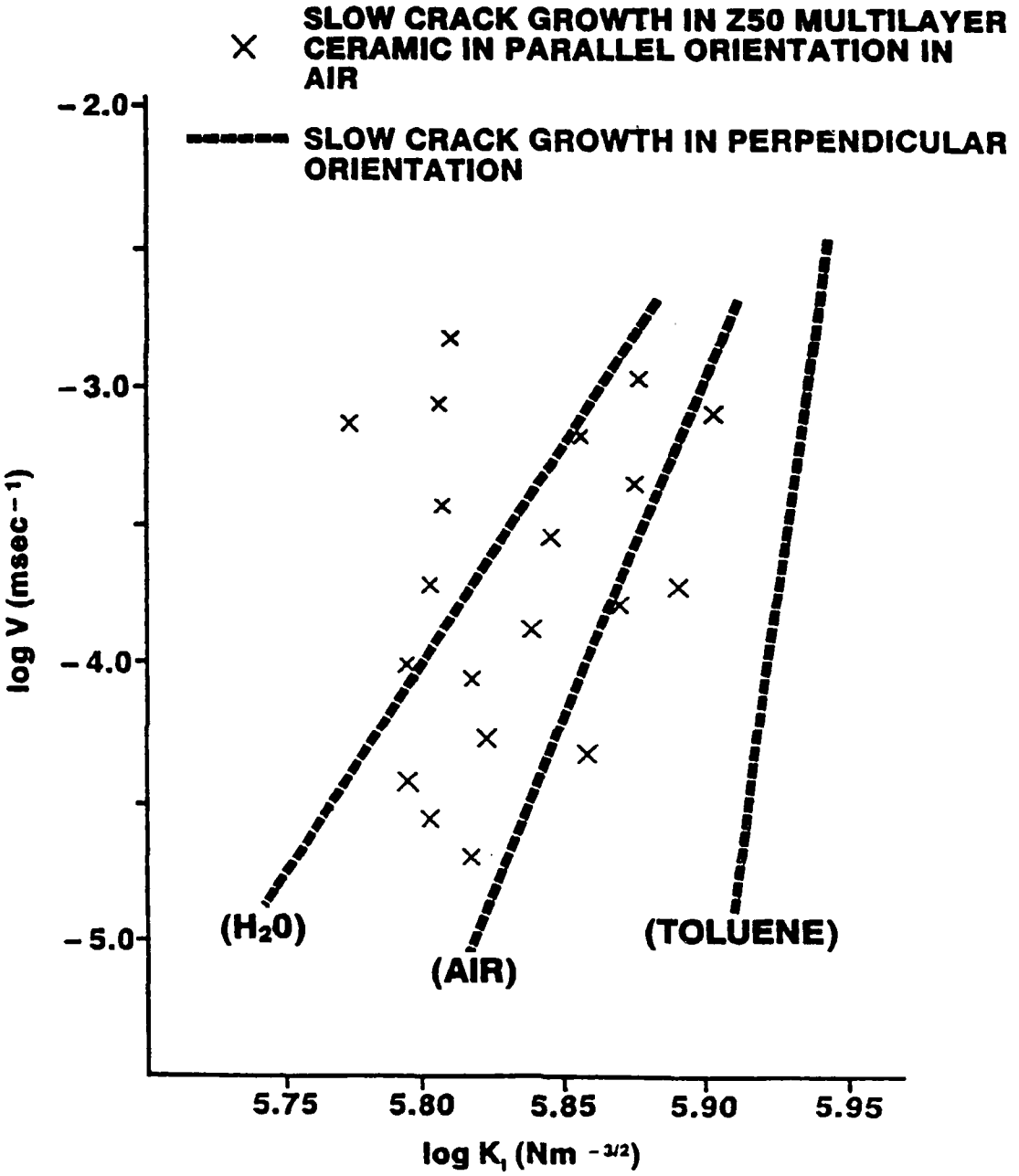

FIGURE 8: EFFECT OF MOISTURE ON SUBCRITICAL CRACK GROWTH IN PARALLEL ORIENTATION

The data points for tests conducted in water and in toluene have not been included but show the same tendency as the data taken in ambient. All of the data taken for this orientation in either ambient, water or toluene exhibit large scatter and tend in some cases to overlap. This degree of scatter in the data is suggested to be a result of the anisotropic macrostructure and the testing orientation. In fact, fracture surfaces from specimens tested in this orientation usually show that at any given time during the experiment, part of the propagating crack resides solely within the ceramic material and part intersects or propagates through the electrode layer. One might expect different crack growth characteristics in different phases. In general, the data do exhibit an overall trend to lower applied stress intensity factors indicating that the crack is able to seek out the path of lowest resistance.

The result of the application of a d.c. electric field to a specimen tested in this orientation is schematically shown in Figure 9. The figure is a trace of a deflection vs. time curve. In this type of specimen with the central web rotated 90^{o} the application of a voltage now establishes an electric field perpendicular to the propagating crack tip. All field strengths were calculated based on the applied voltage and the individual layer thickness of the multilayer body. The generation of an electric field in this orientation serves to retard and eventually stop crack growth as shown in Figure 9. Crack propagation is initiated by the application of a load and then the voltage is applied. At this point a noticeable retardation in crack velocity is observed and within the time span of 20-30 seconds, the crack has stopped entirely. With the load still applied and the voltage removed, the crack once again begins to propagate at a velocity equal (in most cases) to the original velocity. This sequence may be repeated several times on any specimen. In order to reinitiate crack propagation with the voltage still applied, a higher applied load is required and catastrophic failure usually follows. The examination of fracture surfaces has proved inconclusive at this point as to the path that the propagating crack takes during the application and subsequent removal of applied voltages. It may well be that the portion(s) of the crack propagating within the barium titanate layers are impeded by the generation of compressive stresses from the application of electric fields. Such compressive stresses would be oriented in a direction perpendicular to the propagating crack and be expected to impede crack propagation.

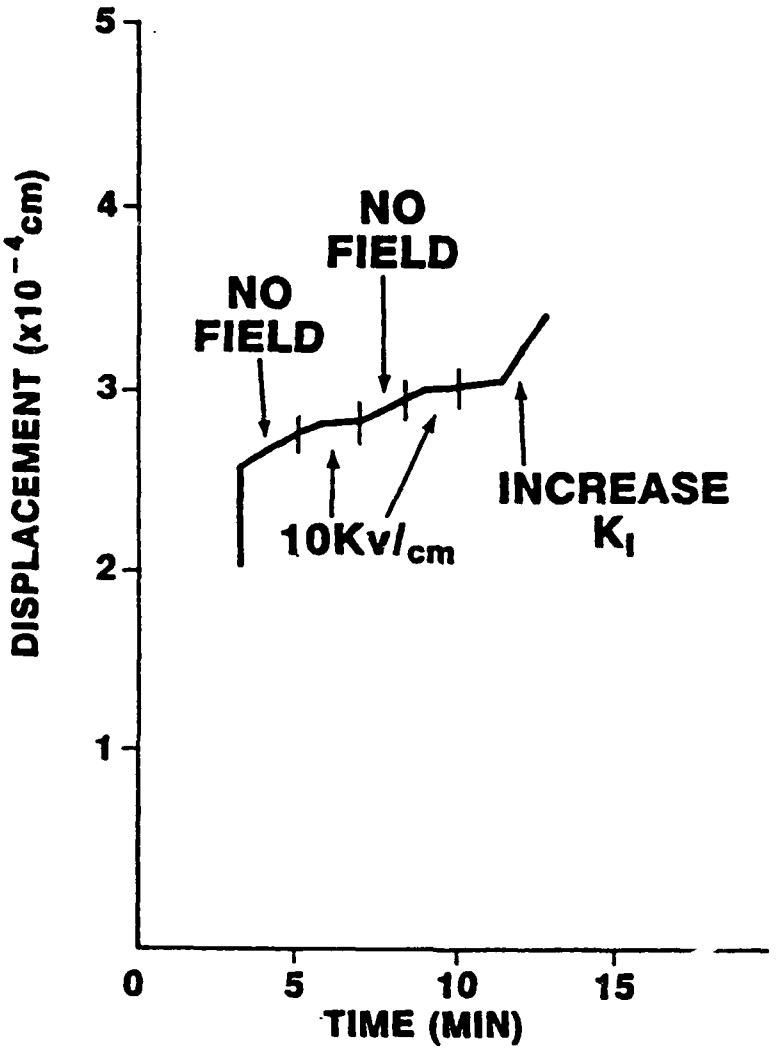

FIGURE 9: EFFECT OF DC FIELD ON SLOW CRACK GROWTH IN PERPENDUCULAR ORIENTATION

C. FRACTURE TOUGHNESS

The fracture toughness values obtained for this material are shown in Table 1. A number of samples were tested in each orientation with the general result being that the fracture toughness of specimens tested in the parallel orientation tends to lower than those in the perpendicular orientation. This supports the slow crack growth data where cracks were seen to propagate at a certain velocity at lower applied stress levels in the parallel orientation. The degree of scatter is not as evident in the fracture toughnesses if one considers just the standard deviations given. The one low value of fracture toughness for Sample #7 in the perpendicular orientation serves to increase the standard deviation of the average.

TABLE 1. FRACTURE TOUGHNESS OF Z5U MULTILAYER CERAMICS AS A FUNCTION OF ORIENTATION

PERPENDICULAR		PARALLEL	
SAMPLE #	$K_{IC}(Nm^{-3/2} \times 10^{-5})$	SAMPLE #	$K_{IC}(Nm^{-3/2} \times 10^{-5})$
2	8.8	37	7.4
7	7.4	39	8.7
10	9.1	40	6.8
11	9.3	41	7.9
14	8.9	45	8.1
16	9.5	49	7.3
17	9.2	54	7.2
18	8.9	55	7.8
AVERAGE = 8.9 ± 0.6		AVERAGE = 7.6 ± 0.6	

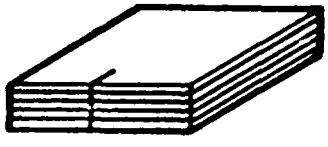

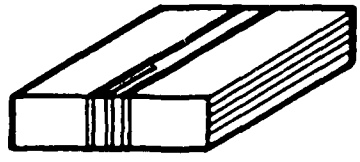

D. MECHANISM

The mechanism whereby crack propagation is hindered in specimens with an electric field applied perpendicular to the crack is postulated to be a phenomenon of electrostriction. This theoretical analysis is currently being developed in conjunction with the Pennsylvania State University Materials Research Laboratory and will be the subject of a future technical report.

IV. CONCLUSIONS

Based on the results obtained thus far, the following conclusions may be drawn.

- Slow crack growth is enhanced in Z5U dielectric capacitor materials when the material is subjected to moisture containing environments.

- Compliance of fracture mechanics specimens does not appear to be effected by orientation of multilayer structure.

- Fracture toughness is higher when crack is oriented perpendicular to the multilayer structure.

- Application of d.c. fields parallel to the crack front does not significantly effect crack growth rates.

- Application of d.c. fields perpendicular to the crack point retards crack propagation possibly due to electrostriction.

REFERENCES

1. E.B. Thornley, Proc. Symp. Capacitor Tech., Appl. and Reliab., Huntsville, Ala., NASA, (24, 25 Feb. 1981) p. 93.

2. R.C. Pohanka, S.W. Freiman and R.W. Rice, Ferroelectrics, 28, 337 (1980).

3. J.G. Bruce, W.W. Gerberich and B.G. Koepke, in Fracture Mechanics of Ceramics, Vol. 4, ed. by R.C. Bradt, D.P.H. Hasselman and F.F. Lange, Pelnum Press, New York, (1978) p. 687.

4. M.J. Cozzolino and G.J. Ewell, IEEE Trans. on Components, Hybrids and Manufacturing Technology, Vol. CHMT-3, No. 2 (1980) p. 250.

5. K.A. Esaklul, K.D. McHenry, B.G. Koepke and H. Vora, to be published. Based on work carried out under contract to Hughes Aircraft Co.

6. A.G. Evans, J. Mater. Sci., 7, 1137 (1972).

7. D.P. Williams and A.G. Evans, J. Testing and Eval, 1, 264 (1973).

8. K.D. McHenry and B.G. Koepke, in Fracture Mechanics of Ceramics, Vol. 5, R.C. Bradt, A.G. Evans, D.P.H. Hasselman and F.F. Lange, Ed., Plenum Press, New York (1983), p. 337.

SECTION 3

W. B. Harrison, K. D. McHenry and B. G. Koepke. Monolithic Multilater Piezoelectric Ceramic Transducers. Honeywell Ceramics Center, Minneapolis, MN, 1986.

MONOLITHIC MULTILAYER PIEZOELECTRIC CERAMIC TRANSDUCERS

W.B. Harrison, K.D. McHenry and B.G. Koepke

Honeywell Ceramics Center, Minneapolis, MN 55428 U.S.A.

ABSTRACT

Cofired multilayer PZT stacks have been under development at Honeywell for potential use in high drive sonar systems. Experimental structures have been produced by electroding cold pressed and tape cast layers with Pt based ink, stacking the layers and firing. After poling, the structures were characterized.

The microstructural characteristics and piezoelectric properties were found to be similar to that observed in bulk PZT of the same composition. The mechanical integrity of these multilayer structures, however, was extremely dependent upon not only microstructural features but also macrostructural features such as electrode design.

INTRODUCTION

Composite multilayer piezoelectric and electrostrictive ceramic structures containing internal electrodes are finding increased use in applications where high electric fields are required for operation. Applications include high power sonar transducers, electromechanical actuators and piezoelectric power supplies. Traditionally, the structures have been produced by bonding electroded ceramic layers with organic adhesives. Where extremely high field strengths (and small electrode separations) are needed, cofired structures with internal electrodes become convenient and, in many instances, required.

Systems benefits resulting from the use of multilayer ceramic structures can be significant. Lower applied voltages can result in the elimination of transformers, minimization of corona discharge and relaxation of overall insulation requirements. In some cases, a multilayer structure is the only way to satisfy applied voltage requirements.

In this paper, results of a program to develop cofired, multilayer PZT structures containing internal electrodes for high drive sonar applications are discussed. Cofired multilayer ceramics are common in the capacitor industry but have only recently been applied in "active" devices [1, 2]. In active devices, mechanical integrity becomes a critical consideration and is addressed in this work. It is now accepted that subcritical crack growth is as common in ferroelectric ceramics as it is in structural ceramics and that the electrical and chemical environments can significantly alter crack growth kinetics. [3-5]. Crack propagation studies have been made on cofired multilayer structures used for this work and the results are discussed in this paper.

FABRICATION

1. General

The general approach used to produce monolithic multilayer PZT stacks is to stack electroded layers into a structure in which the layers can be connected electrically in series as shown in Figure 1. The stack is then fired, usually with intermediate burn-out steps to form a monolithic structure. The electrodes are subsequently connected by firing an electrode on each side as shown in Figure 1.

Two methods have been used to produce monolithic PZT stacks. The first method consisted of producing green ceramic layers by dry pressing. In the second method, the layers were produced by tape casting using a doctor blade technique. In both cases, electrodes were applied by screening metal inks onto the layers. In this work Pt was used for the electrode material.

The process steps used for both methods are shown in Figure 2. Dry pressing is used for thicker parts. A high drive Navy Type III composition with a nominal composition of Fe-doped $Pb_{0.94}Sr_{0.06}Ti_{0.47},Zr_{0.53}O_3$ was used throughout this work. Stacks with outside dimensions of 2.54 X 2.54 X 5.08 cm 0.65mm thick layers were fabricated by both processes and evaluated. The effects of the type of electrode ink on the properties was also evaluated.

2. Dry Pressed Stacks

Spray dried PZT powder was mixed with an organic binder and pressed at 41MPa into large blocks. The binder was burned out at 800°C and the blocks sliced into 0.8mm thick layers that were screened with Pt ink and laminated. The stacks were fired at 1280°C in a closed MgO crucible with excess lead zirconate to maintain the proper atmosphere. Following firing, the ends of the stacks were electroded and refired.

3. Tape Cast Stacks

The slip was prepared by ball milling the powder for 16-18 hours in a temperature controlled room with 25-40 wt/o Cladan No. 73115 binder* using zirconia media. The slip was routinely vacuum deaired before casting. Consistent tape was produced by casting at 0.005-0.1M/S. Pieces suitable for laminating were then punched from the tape and cured for 2 hours at 35°C. Following this treatment, the tape could be stored in closed containers for extended period of time at room temperature.

*Tam Ceramics Inc.,
Niagara Falls, NY 14305

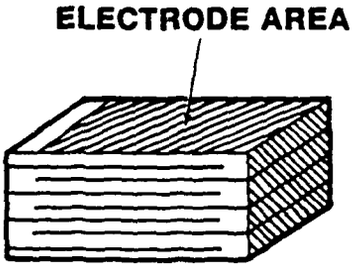

Figure 1: PZT Monolithic Transducer Stack

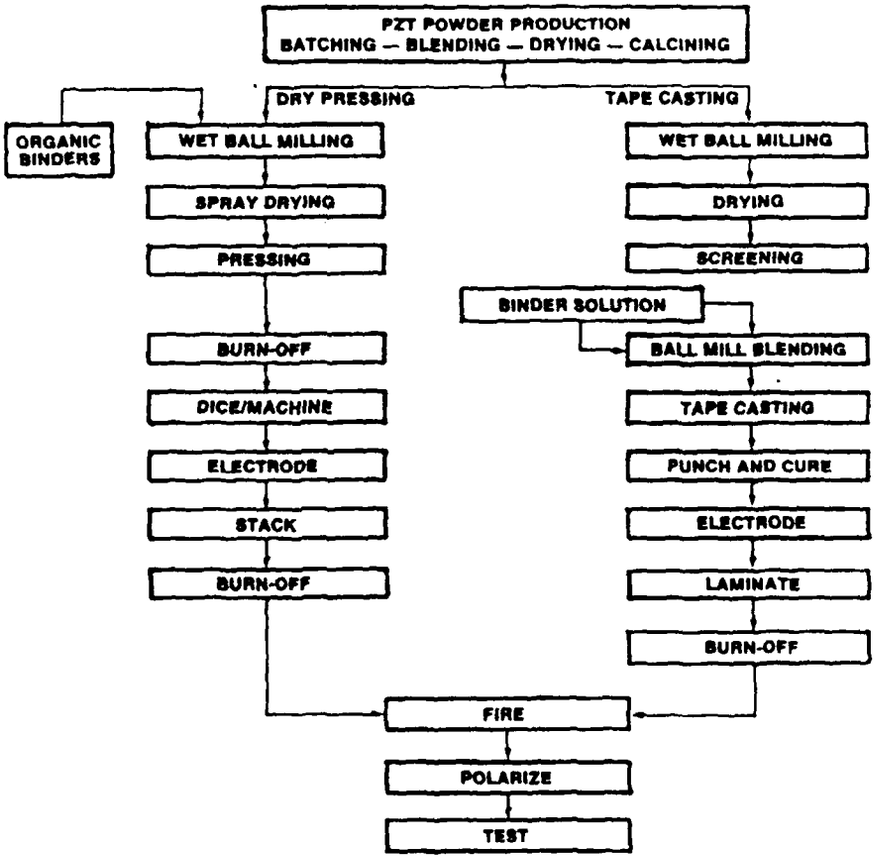

Figure 2: Process Steps for Producing Monolithic PZT Stacks

The layers were then electroded and laminated as before. The thicknesses of the tape cast layers were typically less than that required for proper electrode spacing (i.e., 0.8mm unfired). As a result, alternating layers were electroded. The stack was laminated in a double acting press at approximately 50°C and 12 MPa before burn-off.

The burn-off process turned out to be a critical step in fabricating multilayer PZT stacks. The binder and Pt-filled ink both undergo exothermic reactions upon heating that are presumably enhanced by catalytic action of the Pt. The gas pressure generated can easily destroy the stack. Figure 3 illustrates this phenomenon. The figure shows DTA data measured on a special tape cast laminated stack in which only half the stack contained electrodes. Thermocouples were placed in each half and the temperatures monitored during burn-off. The reaction in the electroded region started earlier during heating, (due, no doubt, to its increased thermal conductivity) and reached a higher temperature presumably due to more reaction. Data such as those shown in Figure 3 allow the thermal cycle to be adjusted to maintain stack integrity during burn-off.

Following burn-off, the tape cast stacks were fired in the same way as the cold pressed. In both cases, after a stack was successfully burned off, no cracking problems were encountered during final firing.

4. Electrode Material Effects

It is well known that the Pt electrode materials contain alloying additions to enhance metallic sintering as well as adhesion to the ceramic. The additions have also been found to alter the sintering kinetics of the PZT to a degree worth mentioning

In a study of the characteristics of electrode inks, a series of experiments were run in which multilayer tape cast stacks were produced using a number of different electrode inks,. The stacks were fired at temperatures from 1080°C to 1280°C. After firing, all parts were poled at 140°C at an electric field of 16 KV/cm. Density, dielectric constant and coupling were measured.

Three electrode inks were used. Type 1, contained substantial amounts (0.3-0.9 wt/o) of Bi, Cd, Cu and Fe. Type 2 contained substantial amounts of Al and Si. Type 3 contained only Bi.

Fired density is plotted as a function of firing temperature for stacks electroded with the three inks in Figure 4. The stacks containing type 1 ink clearly fired to the highest density. The lowest sintering rate was exhibited by stacks electroded with the ink containing only Bi. Dielectric constant followed a similar relation with sintering temperature as density. The piezoelectric properties of stacks all fired at 1280°C were also

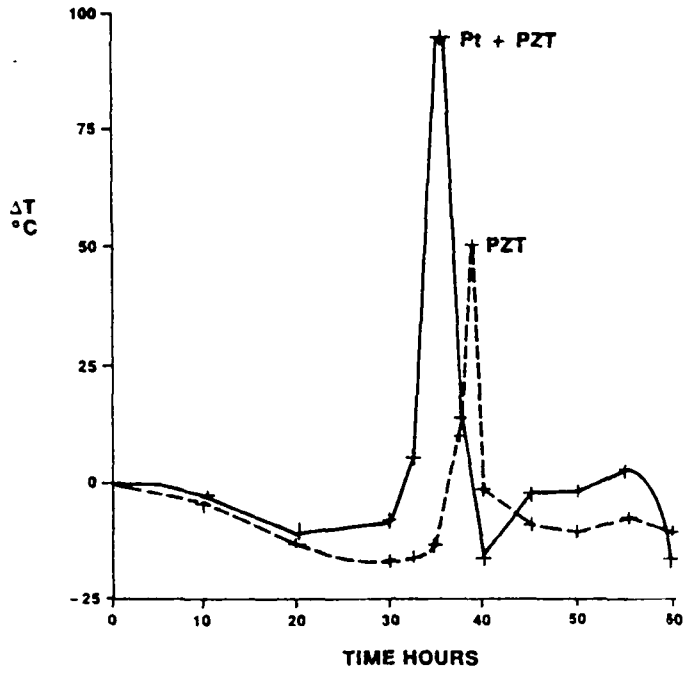

Figure 3: Thermal Analysis of Stack Binder Burn Off

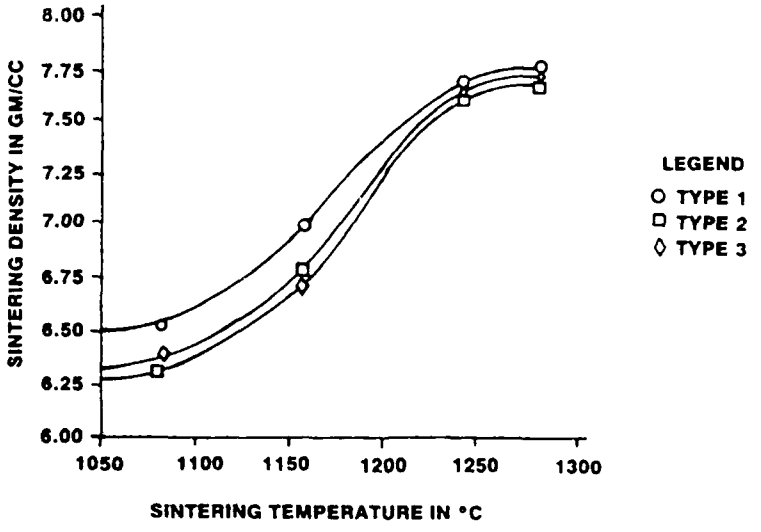

Figure 4: Densification of PZT Stacks with Various Platinum Electrodes

sensitive to the electrode materials. Coupling and dielectric constant were found to increase as the number of layers in a stack increased when Type 1 and Type 2 ink were used. Presumably this behavior is due to the impurity dopants in the inks. When Type 3 ink was used, there was little variation in the piezoelectric properties with the number of layers because of a lower dopant concentration.

As a final point concerning electroding, it was noted that electrode geometry significantly affected burn-off. When the electrode did not extend to the edge of the ceramic layer, a higher incidence of cracking during burn-off was observed. This is presumably due to the fact that the unelectroded regions around the edge of the stack were less permeable to the gases generated during burn-off. As a result, higher internal pressures built up and the stacks fractured.

It may be necessary to fully electrode multilayer stacks for other reasons as well. An electrode that terminates inside a ceramic body is a source of electric field concentration. In piezoelectric and electrostricitive ceramics, this can result in stress concentrations high enough to fracture the parts [2].

CHARACTERIZATION

1. Structures

The characteristic microstructural features of cofired multilayer PZT are evident in the scanning electron micrograph of a fracture surface shown in Figure 5. Porosity in the material is usually homogeneously distributed and consists of fine pores equal to or slightly larger than the grain size. Occasionally large voids such as the one in the lower left hand corner of the micrograph are observed. The grain size as noted from this region is approximately 5-7 microns which is on the order of the electrode thickness. Fracture of this material is typically transgranular.

Figure 6 shows an optical photograph of a surface polished transverse to the layers. The electrode layers are clearly visible. The discolored regions adjacent to the electrode layers are attributed to metallic dopants introduced during the electroding process. The arrows on the right hand side of the micrograph indicate the direction the impurities migrated following application of the electrode layer. The top electrode layer was applied to both surfaces before lamination.

As noted from Figure 6, the impurities migrate considerable distances into the ceramic. We postulate first that this occurs while the ceramic is in the green state and secondly that the impurities that migrate the furthest are in solution (e.g. as organometallic compounds) in the ink.

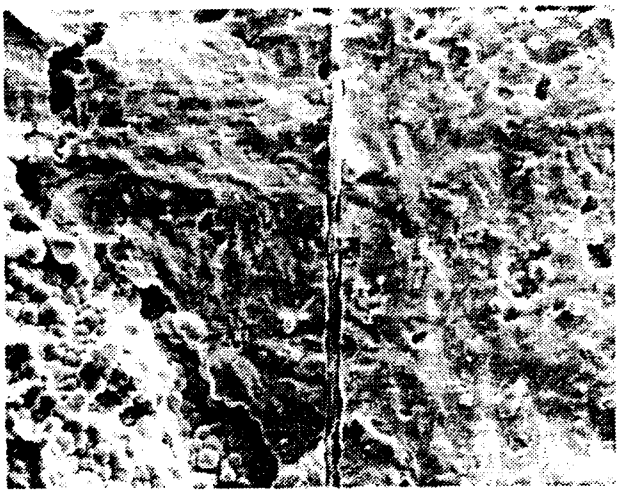

10 μm

Figure 5: Scanning Electron Micrograph of Fracture Surface of Multilayer PZT

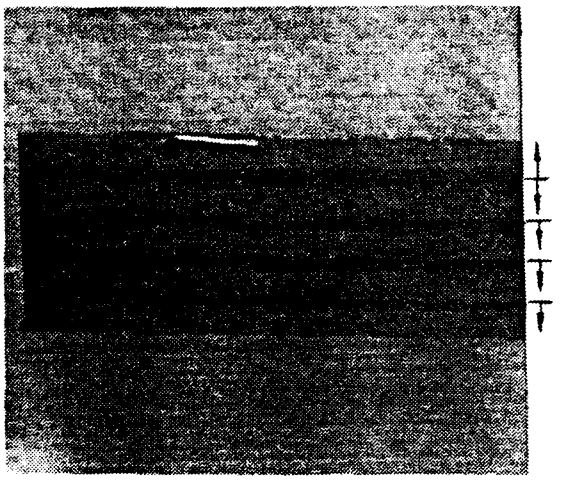

0.2cm

Figure 6: Optical Photograph of Multilayer PZT Macrostructure Indicating Diffusion of Metalic Impurities from the Electrode Layers into the PZT

2. Properties

i) Bulk Properties

The properties of dry pressed and tape cast monolithic stacks with internal platinum electrodes and six active 0.65mm thick layers are compared in Table 1 to bulk PZT with conventional external fired silver electrodes. These data were taken according to Mil Std 1376 recommended procedures.

The unpoled dielectric constant of the monolithic stacks and bulk material were identical to within experimental error. Dielectric constant increased and electrical dissipation decreased with polarization which was typical for this particular PZT composition. Stacks with internal platinum electrodes had higher dissipation than bulk material because of the thinner active layers and the impurities introduced by the platinum sintering aids.

The slightly lower polarization field was used for the tape cast stacks. this caused the frequency constant to be higher and the piezoelectric coupling to be lower than in the dry pressed stacks and bulk PZT. The high field increase in capacitance and electrical dissipation obtained for the tape cast stacks were similar to the dry pressed stacks. These data are typical of the PZT composition used. Since a modified Type III composition was used, the data are not exactly equivalent to Mil Std. 1376 Type III material.

From these data it has been concluded that both monolithic stack techniques can be used to produce satisfactory multilayer piezoelectric structures.

TABLE 1
PROPERTIES OF MONOLITHIC PZT STACKS

Property	Dry Pressed	Tape Cast	Bulk
Relative Dielectric Constant (K^T_3)			
Unpoled	1050	1030	1040
Poled	1240	1200	1233
Dissipation Factor (%)			
Unpoled	0.8	0.5	0.5
Poled	0.6	0.4	0.2
Frequency Constant (N_{31} in HzM)	1600	1640	1600
Piezoelectric Coupling Factor (K_{31})	0.30	0.28	0.30
High Field Increase In Capacitance at 3.9 KV/cm (%)	9.0	9.8	*
High Field Dissipation at 3.9 KV/cm (%)	2.8	2.6	*

*Not Measured

ii) Transducer Properties

A large tape cast monolithic stack (2cm high X 2.54cm wide X 5.08cm long) with 39 active 0.5mm thick layers was produced with the acoustic behavior shown in Figure 7. The admittance magnitude versus frequency and complex admittance plots clearly show the unit was free from spurious resonant points and had minimal mechanical losses. Mechanical Q and K_{31} coupling were 90 and 0.32, respectively. The lower mechanical Q is attributed to the compliance of the platinum layers.

3. Mechanical Integrity

Because the complexity of a multilayer structure may give rise to a variety of processing and structural defects, the mechanical reliability of such components in certain applications becomes highly significant. The generation of V-K_I curves (i.e. crack velocity versus applied stress intensity factor) is a convenient method for determining the mechanical integrity of ceramic materials in various environments. For this work, multilayer PZT samples measuring approximately 5cm X 2.5 cm having 0.6mm thick layers were fabricated for testing by the double torsion technique [6] modified for dead-weight loading [7]. Samples were prepared in two different testing geometries. In one case the crack was oriented perpendicular to the layers in the multilayer structure and in the other case the crack ran parallel to the layers. The results of the fracture mechanics testing are shown in Figures 8 and 9.

In Figure 8, data are shown for samples tested with crack propagation perpendicular to the multilayer structure. The data on the left are for samples tested in water while those on the right (slope of 50) are for tests conducted in toluene, an inert environment with respect to water. It is obvious that the effect of moisture on the mechanical reliability of multilayer PZT, as in the case of most other ceramic oxides, is to enhance subcritical crack growth. This is evidenced by a shift in the curves to lower applied stress intensities with a corresponding decrease in slope (indicating an enhanced stress corrosion susceptibility). These results are similar to behavior noted for bulk 53/47 PZT [3]. From the results shown in Figure 8, there is no observable effect on crack propagation due to poling of the material. This phenomenon is to be expected since in this test geometry the poling direction is parallel to the propagating crack front. Any residual stresses developed as a result of the poling operation should not interact with the crack tip.

In Figure 9 subcritical crack growth results are shown for samples having a multilayer structure parallel to the propagating crack front. In this case, the presence of moisture is seen to also have same deleterious effect on subcritical crack growth. More recent results indicate that moisture enhanced slow crack growth behavior may be accentuated in slightly saline solutions. It is interesting to note that although moisture enhances crack propagation for

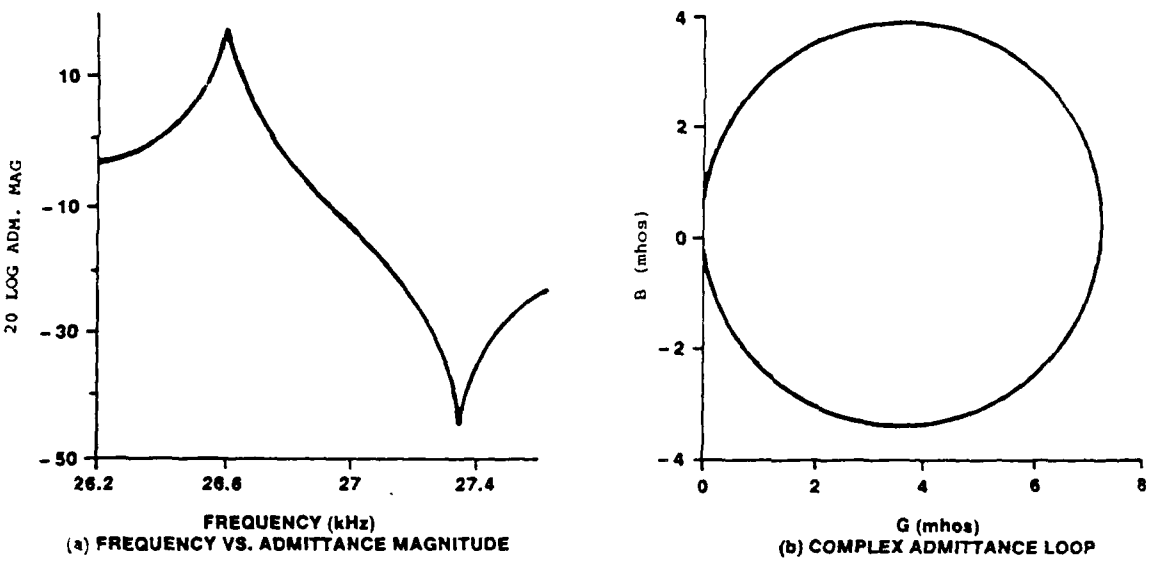

Figure 7: Transducer Behavior of Large Monolithic PZT Stack

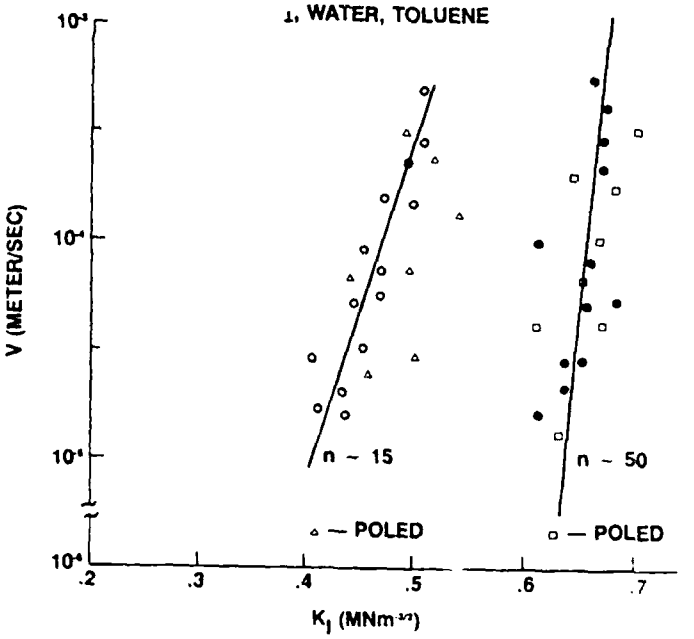

Figure 8: Subcritical Crack Growth Results for Perpendicular Orientation in Multilayer PZT

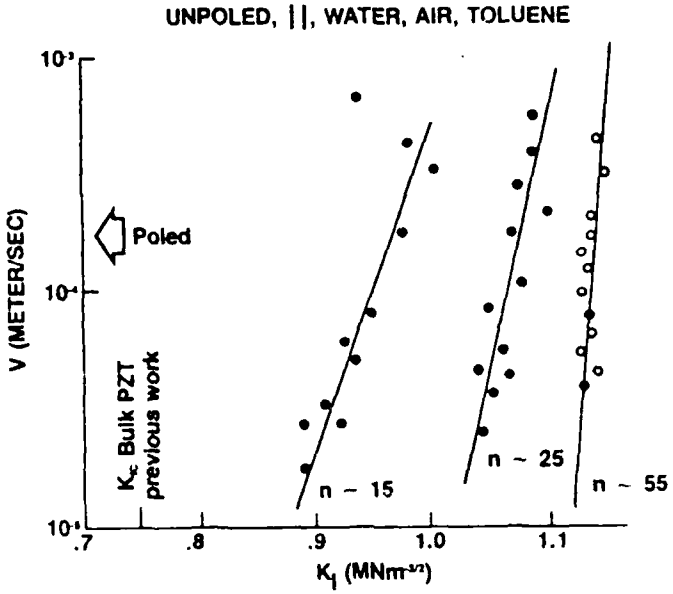

Figure 9: Subcritical Crack Growth Results for Parallel Orientation in Multilayer PZT

both orientations, the results shown in Figure 9 are shifted to higher values of the applied stress intensity. The origin of this apparent "toughening" is not known but may be related to an interaction of the crack with the metallic electrode material. The magnitude of this "toughening" may be observed by comparing the results to the fracture toughness of bulk PZT as indicated.

The mechanical integrity of the poled multilayer material for the parallel orientation was poor and is schematically shown by the large arrow in Figure 9. The slow crack growth results indicated virtually no resistance to fracture. This phenomenon is thought to be a result of mechanical damage introduced during the poling operation as a result of field intensification at electrode terminations within the multilayer structure. More recent results from specimens with full-face electroding indicate improved mechanical integrity.

Overall, the mechanical behavior of these multilayer structures is not dissimilar from that of bulk PZT. More work needs to be done, however, in optimizing the electrode configuration and chemistry to minimize the introduction of potentially critical defects.

SUMMARY

Cofired multilayer PZT structures have been fabricated by electroding and laminating either cold pressed or tape cast layers with Pt based ink. In both cases, the resultant structures exhibit satisfactory microstructural development and bulk property characteristics for use in multilayer piezoelectric applications. The mechanical integrity of such structures as determined from fracture mechanics analysis has been found to be extremely dependent upon electrode design and chemistry. Optimum performance and mechanical integrity of such structures requires full face electroding with an electrode material demonstrating chemical compatibility with PZT.

ACKNOWLEDGMENTS

This work was sponsored by the Office of Naval Research. The continued interest of Dr. R.C. Pohanka is gratefully acknowledged. Much of the work was carried out in collaboration with the Pennsylvania State University Materials Research Laboratory and the Naval Research Laboratory. The authors are indebted to Drs. J. Biggers and G. Dayton from MRL and to Dr. M. Kahn from NRL for technical consultation.

REFERENCES

1. L.S. Bowen, T. Shrout, W.A. Schulze and J.V. Biggers, "Piezoelectric Properties of Internally Electroded PZT Multilayers," Ferroelectrics, Vol. 27, pp. 59-62, 1980.

2. K. Uchino, "Electrostrictive Actuators: Materials and Applications," Bull. Am. Ceram. Soc., Vol. 65, pp. 647-652, 1986.

3. B.G. Koepke and K.D. McHenry, "Fracture and Deformation in PZT," Ferroelectrics, Vol. 28, pp. 343-346, 1980.

4. R.F. Cook, S.W. Freiman, B.R Lawn and R.C. Pohanka, "Fracture of Ferroelectric Ceramics," Ferroelectrics Vol. 50, pp. 593-598, 1983.

5. H. Niitsumg and N. Chubachi, "Fracture Mechanics Parameter and Strength Evaluation of Piezoelectric Ceramic Plate", ibid. pp. 605-610.

6. D.P. Williams and A.G. Evans, "A Sample Method for Studying Slow Crack Growth," J. Testing and Eval., Vol. 1, pp. 264-270 (1973).

7. K.D. McHenry and B.G. Koepke, "Crack Propagation in Z5U Multilayer Dielectrics", To be published.

SECTION 4

K. D. McHenry and B. G. Koepke. Mechanical Reliability of Z5U Multilayer Capacitors. Honeywell Ceramics Center, 5121 Winnetka Avenue North, New Hope, MN, 1986.

MECHANICAL RELIABILITY OF Z5U MULTILAYER CAPACITORS*

KELLY D. MCHENRY AND BARRY G. KOEPKE
Honeywell Ceramics Center, 5121 Winnetka Avenue North,
New Hope, MN 55428

ABSTRACT

Dynamic fatigue experiments were performed on Z5U multilayer capacitors in an attempt to correlate microflaw fracture behavior due to intrinsic processing defects within the material with predictions of fracture behavior based on macrocrack fracture mechanics determinations. A direct correlation between microflaw fracture behavior and predictions based upon macrocrack fracture mechanics techniques was not observable due to the wide size range of processing defects. A systematic post-mortem examination of fracture surfaces was used to identify fracture origins and sort individual test specimens into groups with equivalent flaw sizes. The correlation between microflaw and macrocrack fracture behavior became more obvious after "sorting" the dynamic fatigue data into groups with equivalent flaw sizes.

INTRODUCTION

Multilayer dielectric ceramics offer many advantages over bulk dielectric materials in certain applications. The production of barium titanate based multilayer capacitors is considered to be a mature technology and has provided a direct influence in the development of active piezoelectric multilayer structures. Although these multilayer ceramics offer many performance and system design advantages, the inherent complexity of the multilayer structure coupled with the various processing steps involved during manufacture of these components raise concerns over the long term mechanical reliability. In addition to the conventional types of defects which may be found as a result of processing bulk homogeneous ceramics, the processing of multilayer structures may also introduce a host of unique defects such as delaminations, misregistered electrodes, etc. (1).

Significant information has been generated in recent years concerning the fracture behavior of both bulk and multilayer dielectric materials (2-5). Many of the results are based on fracture mechanics determinations which require the introduction of either a microflaw or a macrocrack by some artificial means. Thus, fracture originates at an artificially induced site instead of at an inherent processing defect. Predictions of fracture behavior for microscopic processing defects based on macrocrack fracture mechanics behavior can be influenced by large structural discontinuties while microflaw behavior is more sensitive to microscopic inhomogenities. The object of the present work was to identify types of processing defects which can cause failure in multilayer Z5U capacitors and to correlate the fracture behavior with that predicted from macrocrack fracture mechanics techniques.

*Work sponsored by the Office of Naval Research

EXPERIMENTAL APPROACH

Multilayer Z5U capacitors measuring 1cm x 1cm x 0.125cm were obtained from Sprague Electric. These capacitors had been sorted by the manufacturer and known to be "bad" units. The external electrode material was removed and each capacitor was cut to yield four test specimens for dynamic fatigue measurements. The final size of each test specimen was approximately 0.50cm x 0.50cm x 0.125cm. A metallic rod was then attached both to the top and bottom faces of the sample through the use of a high-strength epoxy. Actual testing was accomplished by pulling on the metallic rods in a standard testing machine and subjecting individual specimens to uniaxial tension in a direction perpendicular to the laminated structure. Testing was performed at three different strain rates by varying the crosshead speed and at three different temperatures (30, 40, 50°C) in air by placing the sample and rods within a small wire-wound tube furnace.

Previous work (4) had demonstrated the type of fracture behavior observed in Z5U multilayer structures from traditional fracture mechanics techniques. Figure 1 is a summary of slow crack growth results in Z5U capacitor material (not part of the "bad" lot) in several different environments as determined by the double-torsion testing method (6). The results indicate that Z5U multilayer material is susceptible to moisture enhanced slow crack growth in much the same fashion as other ceramic materials. On a logarithmic plot of the crack velocity, V, versus the stress intensity factor, K_I, the slope of the data, n, (i.e. the stress exponent) is an indication of the susceptibility to slow crack growth (low n - greater susceptibility).

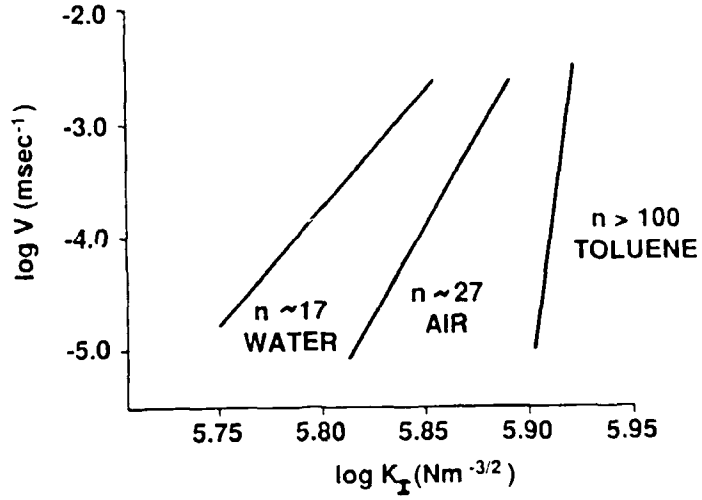

Figure 1: Summary of Slow Crack Growth Results for Z5U Capacitors in Various Environments Using the Double Torsion Testing Technique

The current work made use of dynamic fatigue experiments to assess the fracture behavior caused by processing defects and independently arrive at a value of the stress exponent through the relation (7)

$$\sigma^{n+1} = 2(n+1)E\dot{\epsilon}\sigma_{IC}{}^{n-2}/AY^2K_{IC}{}^{n-2}(n-2) \qquad (1)$$

From this relation a logarithmic plot of the fracture stress versus the strain rate should be a linear result having a slope equal to $1/(n+1)$. A comparison of the value of the stress exponent obtained from the two techniques was used to correlate the fracture behavior.

RESULTS AND DISCUSSION

The dynamic fatigue test results are summarized in Figure 2. The data points represent averages of between 5-7 individual tests at each condition. The confidence limits are not given due to the amount of scatter in the data. 95% confidence limits for any average value depicted in Figure 2 were large enough to encompass all other data points. As a result, attempts to accurately determine values for the stress exponent were unsuccessful. With the lines drawn between the average fracture stress values as shown in Figure 2, values for the stress exponent could range between 2 and 150.

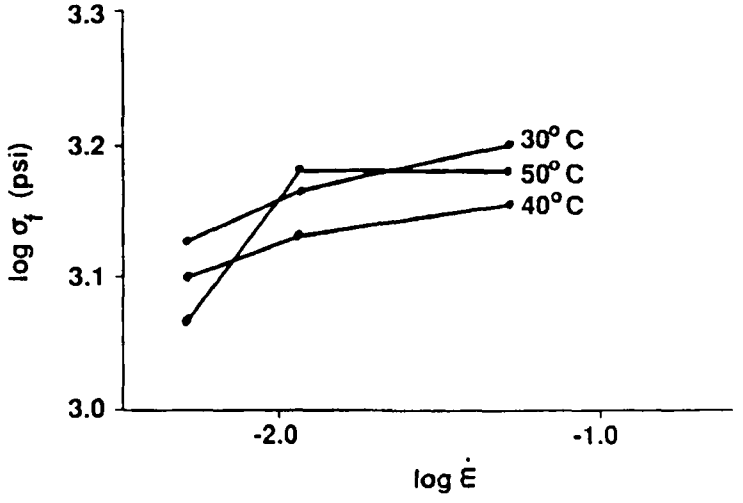

Figure 2: Dynamic Fatigue Test Results for Z5U Capacitors as a Function of Temperature

A presupposition for the successful utilization of this type of analysis is a fairly narrow range in the size of the flaws causing fracture. Scanning electron microscopy of the fracture surfaces to determine fracture origins and the size of the defects indicates that a narrow range of flaw sizes is an invalid presupposition for these tests. In Figure 3, a characteristic fracture surface is indicated showing a uniform distribution of fairly large pores. The multilayer structure is clearly evident with the ceramic layers being approximately 50 microns thick. Another characteristic of the fracture behavior of this material is that fracture was always transgranular in nature. Figure 4 is a higher magnification of one of the individual pores indicating the underlying grain structure having grain sizes of 2-4 microns.

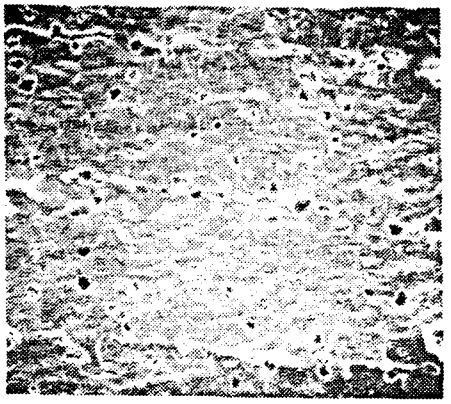

20 μm

Figure 3: Fracture Surface Indicating Large Uniformly Distributed Pores and Multilayer Structure

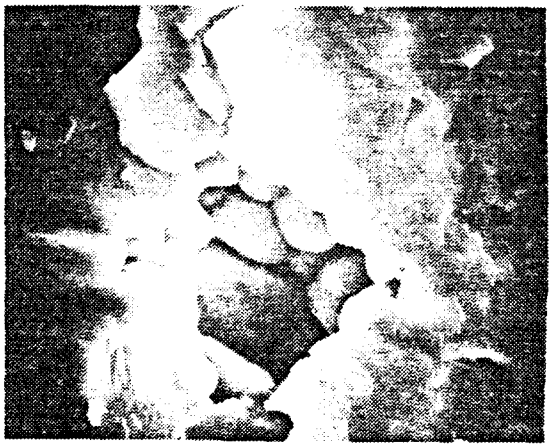

20 μm

Figure 4: Fracture Surface Indicating Pore Structure and Underlying Grain Structure.

Upon examination of the fracture surfaces, a variety of very large defects were discovered. Examples of these are shown in Figures 5 and 6. In Figure 5, the fracture origin for this particular sample is seen to be a large delamination (several hundred microns in size). The sample shown in Figure 6 fractured along an electrode/ceramic interface. The origin of fracture was determined to be the inhomogeneous zone contained within the electrode layer as shown in Figure 6. EDAX identified a high concentration of potassium and chlorine in this region.

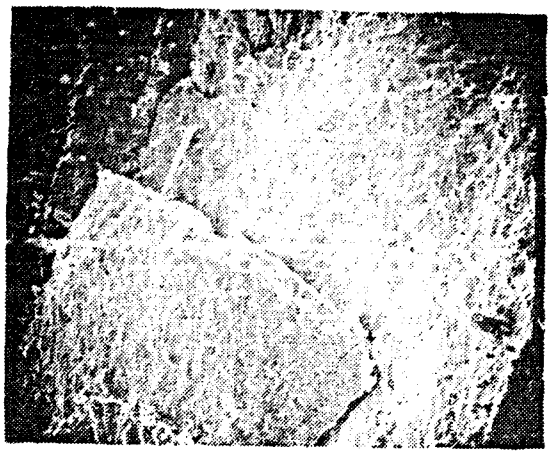

50µm

Figure 5: *Fracture* Surface Indicating Large Delamination and Underlying Crack

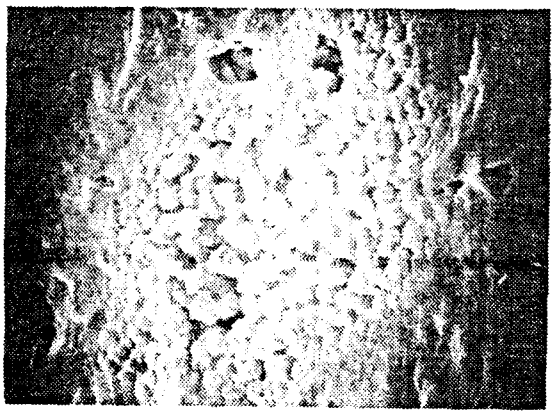

5µm

Figure 6: Fracture Surface Indicating an Inhomogeneous Region in an Electrode Layer. EDAX Analysis Shows a High Concentration of K and Cl.

Subsequent to the microscopic examination of the fracture surfaces, samples were sorted into groups having a more uniform distribution of flaw sizes which governed the fracture behavior. In all cases a very low value of the fracture stress for an individual component could be traced and attributed to a correspondingly large defect. A reevaluation of the data after "sorting" out specimens with gross defects (greater than 40-50 microns) is shown in Figure 7. The resultant slope of the data indicates a value for the stress exponent of approximately 35 which is in fairly good agreement with the predicted value of 27 from macrocrack fracture mechanics tests as seen in Figure 1. The results shown in Figure 7 represent all data collected at the three temperatures and indicate a lack of temperature dependence (30-50^{o}C) for the test results.

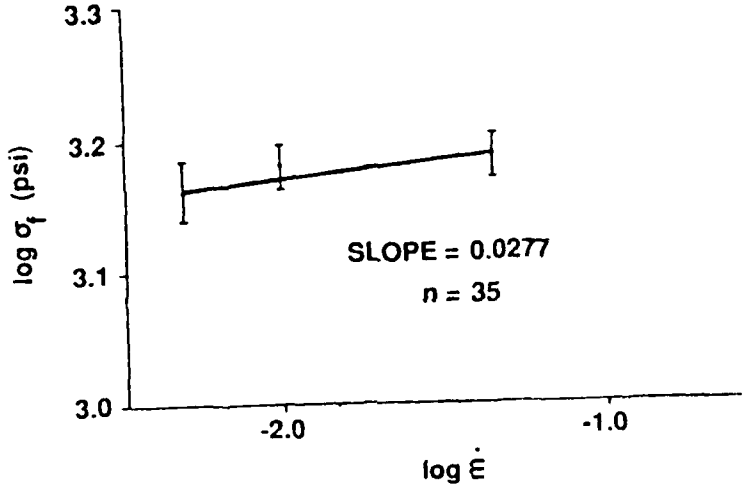

Figure 7: Dynamic Fatigue Test Results for Z5U Capacitors Adjusted to Ensure a More Uniform Flaw Size Distribution

The overall result would thus indicate that macrocrack fracture mechanics techniques may be used to effectively predict intrinsic microflaw behavior of multilayer structures providing a uniform flaw size distribution is assured in the analysis.

CONCLUSIONS

- o A direct correlation between fracture behavior (as measured by microflaw techniques) due to intrinsic processing defects with predictions based on macroflaw fracture mechanics determinations is not possible because of the wide size range of processing defects.

- o A systematic post-mortem examination can be used to effectively "delete" samples with gross defects from the analysis.

- o A correlation between observed microflaw fracture behavior and that predicted by macroflaw techniques becomes more obvious as the data are examined in terms of a "uniform" flaw size population.

REFERENCES

1. E.B. Thornly, in Proceedings of Symposium on Capacitor Technology - Applications and Reliability, Feb. 24-25, 1981, Huntsville, AL, (NASA Publication), P. 93.

2. R.C. Pohnaka, S.W. Freiman, R.W. Rice, Ferroelectrics, 28, 337 (1980).

3. M.J. Cozzolino and G.J. Ewell, IEEE Trans on Components, Hybrids and Manufacturing Technology, Vol. CHMT-3, No. 2 (1980).

4. K.D. McHenry and B.G. Koepke, ONR Technical Report #1, Contract N00014-83-C0141, May 1985.

5. S.W. Freiman (private communication).

6. D.P. Willimas and A.G. Evans, J. Testing and Eva., 1, 264 (1973).

7. S.M. Wiederhorn, in Fracture Mechanics of Ceramics, Vol. 2, (Plenum Press, New York, 1974), p. 623.

SECTION 5

B. G. Koepke, K. D. McHenry, L. M. Seifried and R. J. Stokes. Mechanical Integrity of Piezoelectric and Dielectric Ceramics. Honeywell Ceramics Center, New Hope, MN, 1986.

MECHANICAL INTEGRITY OF PIEZOELECTRIC AND DIELECTRIC CERAMICS

B.G. KOEPKE, K.D. McHENRY, L.M. SEIFRIED AND R.J. STOKES*

HONEYWELL CERAMICS CENTER
NEW HOPE, MN 55428

*HONEYWELL CORPORATE PHYSICAL SCIENCES CENTER
BLOOMINGTON, MN 55420

ABSTRACT

The phenomena of brittle fracture in ceramics and particularly in piezoelectric and dielectric materials is reviewed. Emphasis is placed on both mechanisms of catastrophic failure as well as slow crack growth leading to delayed failure. Material response and component service lifetimes can be strong functions of not only the particular service environment but also material characteristics (both microstructural and macrostructural).

I. INTRODUCTION

The mechanical integrity of piezoelectric ceramic components can be a limiting factor in their service life. This is particularly true in the "active" components such as piezoelectric sonar projectors where severe mechanical stressing occurs during operation. It is also true for "passive" dielectric components such as filters and capacitors which can be inadvertently overstressed during manufacture and installation as well as in service. In all cases, unless proper precautions are taken, tensile stresses may be generated of sufficient magnitude to cause catastrophic failure.

Ceramics generally fail by the propagation of existing flaws either from free surfaces or from internal regions such as bonding interfaces. The larger the flaw, the lower the strength. The fracture strength of a ceramic material may be represented by the classical fracture mechanics relationship:

$$\sigma_f = YK_{IC}a^{-1/2} \qquad (1)$$

where σ_f is the fracture strength, Y is a geometric constant on the order of unity, a is the flaw size, and K_{IC} is the critical value of the stress intensity factor [1]. K_{IC} is a material property (also referred to as the fracture toughness) that defines the resistance to rapid crack propagation. The subscript I in Equation (1) indicates simple tensile loading.

Ceramics also fail through the phenomenon of subcritical crack growth. That is to say, flaws grow slowly at applied stresses less than the critical stress until they reach a value where the conditions of Equation (1) are met. Catastrophic failure then occurs. This subcritical crack growth phenomena is the origin of delayed failure, sometimes called static fatigue. Subcritical crack growth is a general phenomenon in ceramic materials although not always so readily observed as catastrophic fracture. However, its occurrence must be recognized and understood in piezoelectric ceramics if reliable lifetime predictions are to be made. [1, 2]

This paper reviews what is known about the fracture behavior of piezoelectric ceramics. Catastrophic fracture and slow crack growth of both monolithic and multilayer materials are compared in turn.

Processes in the bulk monolithic ceramics are better understood. Even here, however, the fracture process is complicated by residual stresses introduced as a result of the paraelectric to ferroelectric phase transition that occurs when piezoelectric materials are cooled through the Curie temperature.

Multilayer structures are of interest because many piezoelectric components such as piezoelectric actuators and dielectric multilayer ceramic capacitors are deliberately made with this structure. In multilayer structures, the additional feature of structural anisotropy is introduced and must be accounted for as well as the other sources of internal stress noted above. It will become evident that much work needs to be done on the multilayer materials before reliable lifetime predictions can be realized.

II. MONOLITHIC PIEZOELECTRIC CERAMICS

A. Fracture

Table 1 compares typical values of strength and fracture toughness for common materials with those of the piezoelectric ceramic, lead zirconate titanate (PZT).

Metals have high strengths and toughness. Polymers typically have low fracture strengths but are comparably tough. As a class, ceramics have low values of toughness (approximately 1-2 orders of magnitude less than steel). Since their strengths depend on flaw size according to Equation 1, values for a particular ceramic vary and depend on extrinsic variables such as surface finish. Piezoelectric ceramics have a fracture strength and toughness comparable to glass. Thus we note at the outset that PZT is a brittle material.

In contrast to other brittle ceramics, however, the fracture process in piezoelectric ceramics depends on temperature, composition, and microstructure in ways that are all related to the paraelectric/ferroelectric transformation these materials undergo at the Curie temperature. The bulk properties in the paraelectric and ferroelectric states are quite different. Pohanka, et al. [3-6] have shown in an extensive series of studies on $BaTiO_3$ and PZT that fracture toughness is greatest in the ferroelectric state and that fracture strength is greatest in the paraelectric state for materials with equivalent flaw sizes. These results lead to the conclusion that microstructural inhomogeneities (internal stress, twinning, microcracking, etc.) introduced during the transformation play a dominant role in the fracture process

Table 1. Comparison of Typical Mechanical Properties of Common Materials*

Material	Fracture Toughness $K_{IC}(MPam^{1/2})$	Fracture Strength $\sigma_f(MPa)$
Steel (4340)	60	1515
Aluminum (2024-T651)	24.2	455
Polymer (polystyrene)	2	40
Al_2O_3	2.3	276
PZT	.75	138
Glass (silica)	.75	69

*Data taken from various materials handbooks

The effects of grain size on fracture were also studied. Figure 1 shows the variation of fracture toughness (K_{IC}) with grain size for $BaTiO_3$ and PZT in the ferroelectric and paraelectric states. Toughness increases with grain size in the ferroelectric state to a grain size of approximately 50 μm. The incidence of both twins (i.e. domain boundaries) and microcracks introduced by the paraelectric/ferroelectric phase transformation increases with grain size. Interaction of a crack with twins and microcracks accounts for the increase in toughness in materials with moderate grain sizes [5]. At larger grain sizes, microcracks dominate and the toughness drops off [7]. In the cubic paraelectric state these features are absent and toughness is not expected to be a function of grain size [5, 8].

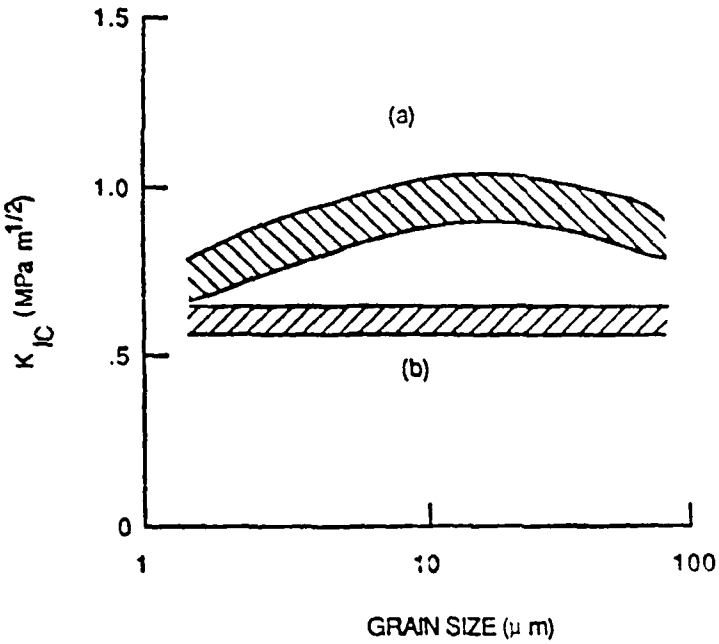

Figure 1: Plot showing K_{IC} as a function of grain size for $BaTiO_3$ and PZT [4] at room temperature (RT) and at 150°C. The materials are ferroelectric at RT and paraelectric at 150°C.

Poling a piezoelectric ceramic also introduces internal stresses and imparts an anisotropy that affects fracture behavior. Specifically, fracture toughness is lower for cracks propagating on planes perpendicular to the poling direction [9, 11]. The difference in toughness for cracks propagating parallel and perpendicular to the poling direction can be as high as a factor of two in PZT [9]. The anisotropy (in particular the elastic anisotropy) must be taken into consideration when describing the fracture behavior, otherwise erroneous conclusions can be reached concerning the magnitude of the toughness [9, 12]. Poling introduces anisotropy at the microstructural level. Anisotropy in the multilayer ceramics discussed later at the macrostructure level will also be shown to affect fracture behavior.

The above investigations have indicated that crack propagation in piezoelectric ceramics is sensitive to the displacive paraelectric/ferroelectric phase transformation and the internal stresses associated with it. Pohanka et al. [4] have suggested that equation (1) needs to be modified to take the internal stress into account as follows:

$$\sigma_f(F.E.) + \langle\sigma_i\rangle = Y\, K_{IC}\,(F.E.)a^{-1/2} \qquad (2)$$

where $< \sigma_i >$ is an average of internal stresses acting perpendicular to a critical flaw and K_{IC} (F.E.) is the fracture toughness in the ferroelectric state. Since internal stresses are absent in the paraelectric state

$$\sigma_f(\text{P.E.}) = Y\, K_{IC}\,(\text{P.E.})a^{-1/2} \tag{3}$$

The two equations can be solved simultaneously to determine the internal stress

$$<\sigma_i> = \sigma_f(\text{P.E.}) \frac{K_{IC}(\text{F.E.})}{K_{IC}(\text{P.E.})} - \sigma_f(\text{F.E.}) \tag{4}$$

In this way, internal stresses can be estimated from strength and fracture toughness data taken above and below the Curie temperature. Internal tensile stresses for PZT and $BaTiO_3$ samples with flaw sizes on the order of 25 μm were calculated to be $\sim$ 25 MPa. This is a measurable and not unreasonable value in light of the fracture strength data in Table 1. Since the internal stresses are averaged over the flaw size, the effect diminishes at larger grain (and flaw) sizes.

The most useful piezoelectric compositions from a sonar efficiency point of view, are those close to phase boundaries in their respective phase diagrams, where the structures and properties are most sensitive to composition. Pohanka et al. [5] have measured the fracture toughness of a number of PZT compositions near the morphotropic boundary at 53.5 $PbZrO_3$- 46.5 $PbTiO_3$ (see Figure 2). A definite minimum in toughness was observed on the phase boundary. These data are shown in Table 2.

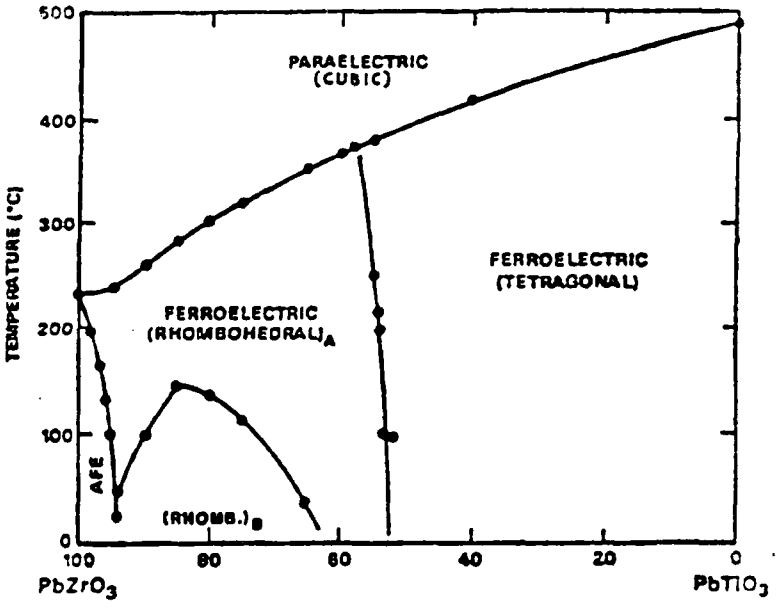

Figure 2: $PbZrO_3$ - $PbTiO_3$ Phase Diagram [5, 7]

Table 2. PZT Fracture Data [5]

Composition	Crystal	K_{IC}	Strength
$Pb(Zr, Ti)O_3$	Structure	$MPam^{1/2}$	MPa
56/44	Rhombohedral	1.52	163
53.5/46.5	Mixed	1.00	68
50/50	Tetragonal	1.51	104

The origin of this minimum in fracture toughness at the morphotrophic boundary in PZT is not clear at this time. Pohanka et al. [5] suggest the effect results from a number of competing toughening mechanisms including microcracking in the tetragonal phase, stress assisted phase transformations in the rhobohedral material, decreased internal stresses due to a higher number of twin states in compositions near the morphotrophic boundary, and others.

To summarize, the fracture behaviors of the piezoelectric ceramics $BaTiO_3$ and PZT are similar and fairly well understood. In most cases, the strengths in the paraelectric state are greater than those cooled through the Curie temperature*. This behavior is attributed to localized residual tensile stresses in the ferroelectric material. In fine grained samples (g.s. <5 μm), the toughness of both paraelectric and ferroelectric modifications are similar. At larger grain sizes ferroelectric twins (i.e. domain boundaries) and microcracks are prominant obstacles to crack propagation and the toughness increases with grain size. At even larger grain sizes. toughness decreases as single crystal behavior is approached.

B. Subcritical Crack Growth

Delayed catastrophic failure in piezoelectric ceramic components usually results from subcritical crack growth. Information on the kinetics of the process are needed to predict lifetimes Subcritical crack growth is a general phenomenon in ceramics and a unique relationship has been found between crack velocity and stress intensity factor [1, 2]. This relationship is shown schematically in Figure 3. Four loading regions are observed. First, a static fatigue limit, K_0 may exist below which crack growth is absent. Second, at higher values of K_I, V increases as K_I^n where n is a constant (Region I). Third, V typically levels off over a limited range of K_I, (Region II) and finally rises rapidly in Region III. When the applied stress intensity factor reaches the critical value, K_{IC}, catastrophic fracture occurs.

---

*These results are not universal. Grekov and Kramarov [13] report an increase in strength when some piezoelectric ceramics are cooled through the Curie temperature. The situation is complicated and warrants further study.

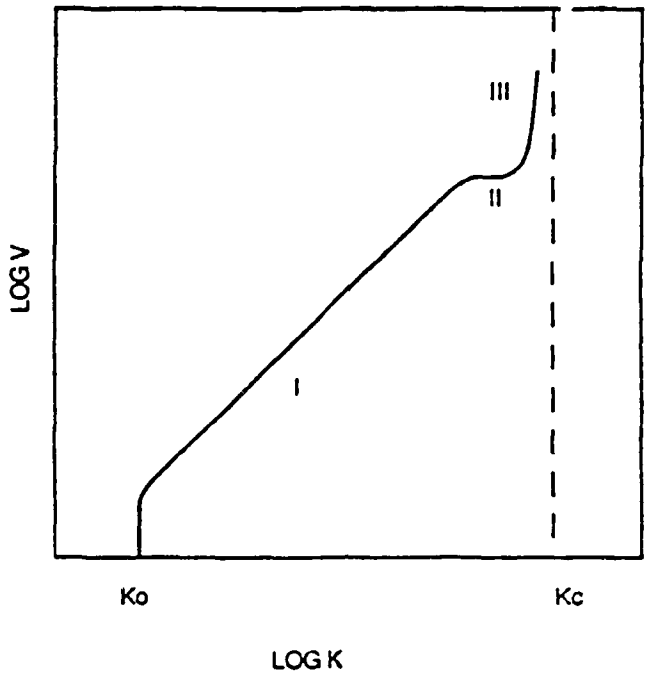

Figure 3: Schematic showing different regions of slow crack growth behavior on a velocity, V, stress intensity factor, K, diagram.

Failure can be predicted if the initial flaw size and the operating stresses are known and if the crack growth velocity--stress intensity factor ($V\text{-}K_I$) relation for the material has been measured. Furthermore, since slow crack growth depends sensitively on the environment, it is necessary to know the $V\text{-}K_I$ curves for each environment. Bruce et al. [12] made extensive measurements of the effects of environment on subcritical crack growth in PZT. They compared the effects of water, toluene, Freon, and mineral oil environments as shown in Figure 4. Water significantly enhanced the slow fracture of PZT. The data can be discussed in terms of the different regions of the $V\text{-}K_I$ curve illustrated in Figure 3. The measurements made in water never depart from Region I, they exhibit the highest crack velocities and the greatest sensitivity to stress intensity factor. Water free environments such as toluene, Freon, and mineral oil result in less subcritical crack growth. Toluene shows all three Regions, while Freon and mineral oil show no crack growth until the stress intensity factor reaches a level high enough to be in Region III. The fracture toughness, K_{IC}, for PZT is also indicated on Figure 4. These data confirm that environmental effects can be very significant. For example, at equivalent stress intensity factors, the crack velocity can be many orders of magnitude less in an inert (mineral oil) than in an active (water) chemical environment.

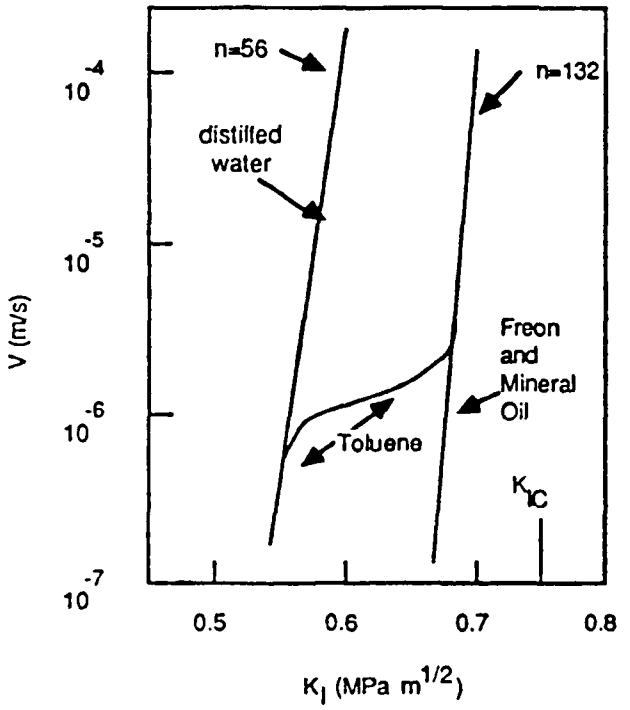

Figure 4: Crack velocity in unpoled PZT measured as a function of applied stress intensity factor in a number of environments at room temperature. Curves for poled PZT were similar.

There is another environmental effect to be taken into consideration in dielectric ceramics and this is the applied electric field. Consider a crack propagating in an electrostrictive material in an electric field. Since a crack is a discontinuity, there will be a field concentration at the crack tip. The material in this region will expand more than its surroundings and, as a consequence, will be placed in compression. A compressive stress field reduces crack propagation and can stop the slow crack growth altogether. This effect has been studied in a number of dielectric materials by the authors [14] and others [15].

The situation in piezoelectric ceramics is subtle because of the magnitude of the piezoelectric strain compared to electrostrictive strain and the directionality of the strain in poled materials. Indeed, McHenry and Koepke [16] found that applied fields significantly increase crack propagation in PZT. Figure 5 reproduces V-K_I curves for unpoled PZT samples to which an a.c. (2KHz) field was applied perpendicular to the plane of the propagating crack. Crack velocities are seen to increase as this electric field increases. The effect was found to be independent of frequency and, in fact, was also observed with a d.c field.

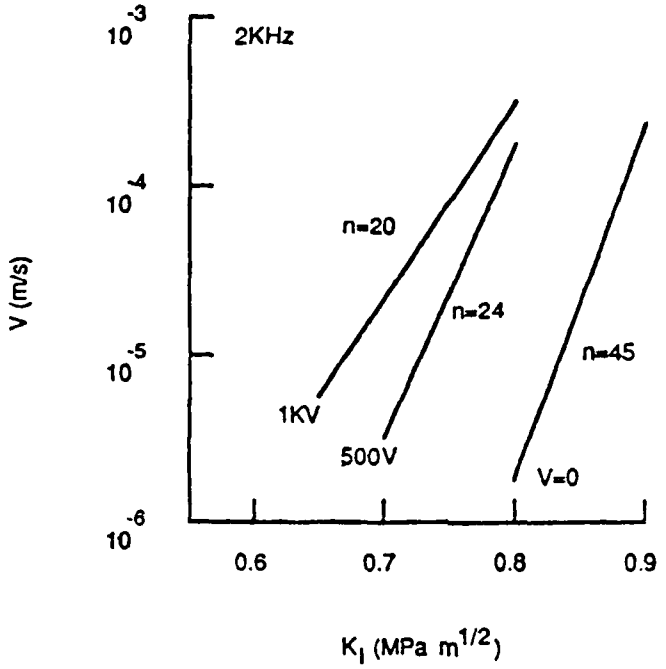

Figure 5: Effect of applied A.C. field on crack propagation in unpoled PZT.

For poled PZT, the application of electric fields parallel with the poling direction and perpendicular to the crack plane always caused the crack to deviate in a direction against the poling direction. It is suggested that in this instance the stresses generated by the field concentration at the crack tip are shear stresses as a result of the material's 4mm crystal symmetry, causing mixed mode loading on the crack. [16]

In summary, piezoelectric ceramics such as PZT and $BaTiO_3$ have a tendency for subcritical crack growth that is enhanced by environments containing water and by applied electric fields. It is, therefore, essential that the fracture processes in piezoelectric and dielectric materials be analyzed, in order that components may be designed for application in a wide range of service environments.

III. MULTILAYER PIEZOELECTRIC AND DIELECTRIC CERAMICS

A. Fracture

The additional complexity of a multilayer structure gives rise inevitably to processing and structural defects not associated with monolithic homogeneous ceramic bodies. An example could be delamination of an electrode/ceramic interface due to chemical incompatibility or poor adhesion between the electrode and the ceramic material. This, and other defects, may arise in the original processing or, subsequently, during fabrication and rework. [17]

In multilayer piezoelectric composites cracks tend to follow the plane of the internal electrodes. Again, this is an example of anisotropy in fracture behavior which is a consequence of structural (and elastic) anisotropy. This may be recognized when the fracture toughness of Z5U capacitors is measured as a function of orientation. The fracture toughness of Z5U $BaTiO_3$ capacitors is approximately 20% higher (0.89 $MPam^{1/2}$ versus 0.76 $MPam^{1/2}$) when measured perpendicular to the multilayer structure [14]. Presumably, the crack front interacts with the electrode layers in a manner similar to the mechanism operative in dispersion strengthening. That is, the electrode layer deforms and absorbs elastic strain energy concentrated at the crack tip.

Figure 6 is a scanning electron micrograph of a fracture surface of a Z5U $BaTiO_3$ capacitor [18]. The fracture occurred when the capacitor was being loaded for a dynamic fatigue test. The fracture origin is the delaminated region located in the lower center of the photograph. The delamination (several hundred microns in extent) can be typical of defects encountered in capacitor structures. This particular defect was a result of the original manufacturing process.

The presence of defects is sufficient to cause fracture of multilayer capacitors due to thermal stresses. Cozzolino and Ewell [17] have shown that very small cracks or defects may lead to premature fracture of capacitors due to thermal stresses introduced by the reflow soldering operation used to attach the components directly to a board. It has been estimated that such stresses may typically reach 80 MPa depending on location.

The importance of proper design considerations in the attachment of capacitors to boards has been emphasized by Van Den Avyle and Mecholsky [19]. They quote an example where the change to a stronger and more creep resistant solder resulted in the fracture of capacitors having twice the fracture toughness of capacitors which were successfully soldered with a more compliant alloy.

In summary, the mechanism(s) of failure and the characteristics of the fracture process (e.g. delamination) in multilayer ceramics differ from those observed in the bulk form. The differences are primarily due to a combination of structural anisotropy and elastic anisotropy.

Figure 6: Scanning electron micrograph of fracture surface of Z5U multilayer capacitor indicating fracture origin at site of interfacial delamination.

B. Subcritical Crack Growth

Further evidence of the anisotropic effects on fracture behavior in multilayer dielectrics is obtained from measurements on slow crack growth to be described next for both Z5U $BaTiO_3$ capacitors and multilayer PZT. We emphasize here that certain results are expected to be different because of basic differences in the materials. The capacitor material is paraelectric and is not expected to react to an electric field in the same way PZT (or piezoelectric $BaTiO_3$) will.

1. Multilayer Z5U Capacitors

Evidence of subcritical crack growth in Z5U multilayer capacitors under ambient conditions comes indirectly from the dynamic fatigue results shown in Figure 7 [18]. In a dynamic fatigue test, fracture strength is measured as a function of loading rate. Since subcritical flaw growth occurs during loading, and strength is inversely proportional to the square root of the flaw size (Equation 1), higher strengths are realized at faster loading rates. Thus the effect of subcritical crack growth can be inferred from the strain rate dependence of the fracture stress. For the data shown in Figure 7, the resultant slope (given as $1/n+1$) yields a value for the stress exponent, n, (the same n as in Figure 3) of approximately 35. This is in good agreement with macroscopic fracture mechanics determinations for the same material [14].

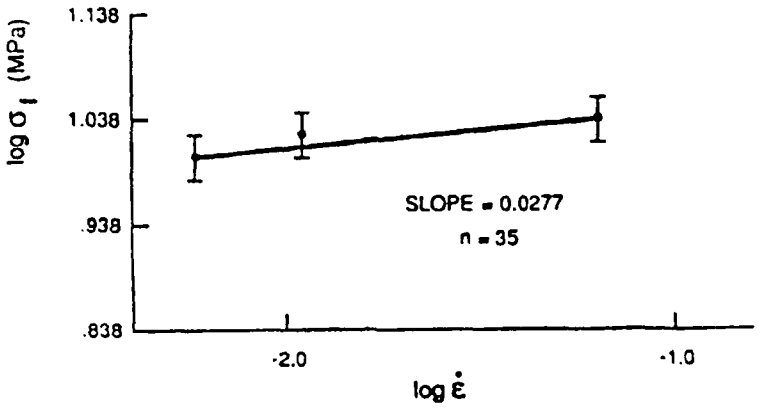

Figure 7: Room temperature dynamic fatigue results for Z5U multilayer capacitors with the applied stress perpendicular to the multilayer structure.

The subcritical crack growth characteristics of multilayer materials vary with orientation, environment and electric field. With respect to orientation, crack growth is "easier" for a given environment if crack propagation is parallel to the multilayer microstructure. With respect to the environment, moisture is found to enhance subcritical crack growth in multilayer Z5U capacitors much the same as in other oxide ceramics. The overall effect is to reduce the stress exponent, n, from values $\sim$100 when testing in "moisture-free" environments such as toluene to values $\sim$20 when tested in aqueous environments [14]. Such results indicate a potentially limited lifetime of components subjected to moisture containing environments if stressed during service.

Subcritical crack growth characteristics vary in electric field environments because of the electrostrictive nature of Z5U material coupled with the anisotropic macrostructure of the multilayer components. An application of high dc fields may result in no effect on subcritical crack growth or, in some cases, retardation or cessation of crack growth depending upon the orientation of the applied field with respect to the propagating crack. When high dc fields are applied perpendicular to a propagating crack, crack growth is retarded due to the generation of compressive stresses from electrostriction When a high dc field is applied in a parallel direction to the crack front, no interaction with the propagating crack has been observed.

2. Multilayer PZT

In Figure 8, data are shown for multilayer PZT samples tested with crack propagation occurring perpendicular to the multilayer structure. The data on the left are for samples tested in water while those on the right (slope of 50) are for tests conducted in toluene, an inert environment with respect to water. It is obvious that the effect of moisture on crack propagation in multilayer PZT is to enhance subcritical crack growth. This is evidenced by a shift in the curves to lower applied stress intensities with a corresponding decrease in slope. These results are similar to behavior noted for bulk 53/47 PZT [12, 20].

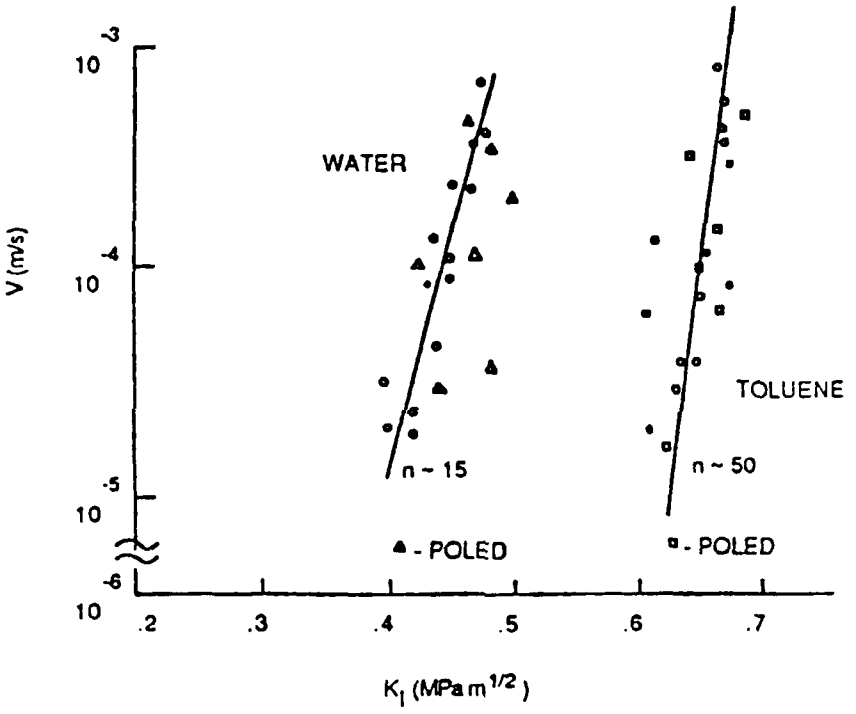

Figure 8: Subcritical crack growth results for perpendicular orientation in multilayer PZT.

In Figure 9, subcritical crack growth results are shown for samples having a multilayer structure parallel to the propagating crack front. In this case, the presence of moisture is seen also to have the same deleterious effect on subcritical crack velocity. More recent results indicate that the sensitivity to moisture may be further accentuated by slightly saline solutions [14].

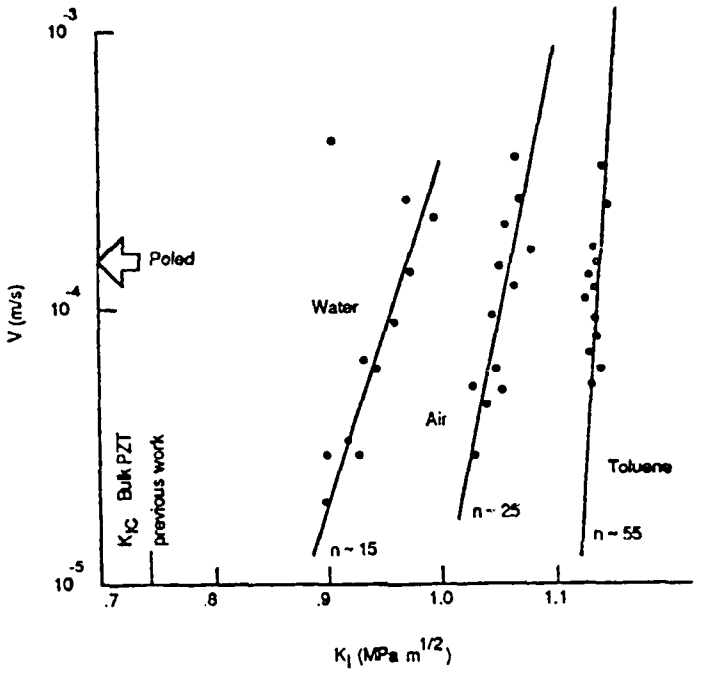

Figure 9: Subcritical crack growth results for parallel orientation in multilayer PZT

It is interesting to note that while moisture enhances crack propagation for both orientations, the results shown in Figure 9 are shifted to higher values of the applied stress intensity. The origin of this apparent "toughening" for the parallel orientation is not known but may be related to the metallic electrodes.

The mechanical integrity of poled multilayer PZT for cracks propagating parallel to the layers was very poor and is represented by the large arrow in Figure 9. The data fall well off the scale of the graph. The slow crack growth measurements indicated virtually no resistance to fracture (K_I<0.1 MPam$^{1/2}$. This degradation is thought to be a result of excessive mechanical damage (microcracking and/or delamination) introduced during the poling operation where the interdigited electrodes terminated within the multilayer structure. More recent results with full face electroding indicate much improved mechanical integrity.

Overall, slow crack growth in multilayer $BaTiO_3$ and PZT structures exhibits similar responses to environment and field as the bulk material. More work needs to be done, however, in understanding the crack/structure interaction and in optimizing the electrode configuration and chemistry to minimize the interfacial defects.

SUMMARY

The mechanical behavior of piezoelectric (and one dielectric) ceramics has been reviewed. Fracture has been shown to depend on fracture toughness and flaw size in a predictable fashion. The concept of subcritical crack growth was introduced and shown, particularly in piezoelectric ceramics, to depend sensitively on the environment. Chemical and electrical environments can significantly alter slow crack growth in these materials. Poled piezoelectric ceramics and multilayer structures exhibit structure and elastic anisotropy that alter crack propagation characteristics. Water enhances crack propagation. In piezoelectric ceramics electric fields enhance crack growth. In electrostrictive ceramics (e.g. paraelectric $BaTiO_3$) cracks are stopped by the application of an electric field. These effects (particularly in piezoelectric ceramics) are subtle and not clearly understood, but will affect component lifetime and will have to be considered if lifetime prediction or enhancement becomes a required feature.

ACKNOWLEDGMENTS

Portions of this work were supported by the Office of Naval Research. The authors are indebted to Dr. R.C. Pohanka for his continued interest and for stimulating technical discussions. Dr. S.W. Freiman is acknowledged for his critical review of the manuscript.

REFERENCES

1. A.G. Evans and T.G. Langdon, Prog. in Mater. Sci., 21, 187 (1976).

2. S.M. Wiederhorn, in Fracture Mechanics of Ceramics, Vol. 2, R.C. Bradt, D.P.H. Hasselman and F.F. Lange, ed. Plenum New York (1974) p. 613.

3. R.C. Pohanka, S.W. Freiman and B.A. Bender, Journ. Amer. Ceram. Soc., 61, 72 (1978).

4. R.C. Pohanka, S.W. Freiman and R.W. Rice, Ferroelectrics, 28, 337 (1980).

5. R.C. Pohanka, S.W. Freiman, K. Okazaki and S. Tashiro, in Fracture Mechanics of Ceramics, Vol. 5, R.C. Bradt, A.G. Evans, D.P.H. Hasselman and F.F. Lange eds. Plenum, New York (1983) p. 353.

6. R.F. Cook, S.W. Freiman, B.R. Lawn and R.C. Pohanka, Ferroelectrics, 50, 267 (1983).

7. B. Jaffe, W. Cook Jr. and H. Jaffe, Piezoelectric Ceramics, Academic Press, New York (1971).

8. R.W. Rice, S.W. Freiman and P.F. Becher, Journ. Amer. Ceram. Soc., 64, 345 (1981).

9. G.G. Pisarenko, V.M. Chusliko and S.P. Kovalev, Journ. Amer. Ceram. Soc., 68, 259 (i985).

10. T. Yamamato, H. Igarashi and K. Okazaki, Ferroelectrics, 50, 273 (1980).

11. K. Okazaki, Bull. Amer. Ceram. Soc., 63, 1151 (1984).

12. J.G. Bruce, W.W. Gerberich and B.G. Koepke, in Fracture Mechanics of Ceramics, Vol. 4, R.C. Bradt, D.P.H. Hasselman and F.F. Lange, eds., Plenum, New York (1978) p. 687.

13. A.A. Grekov and S.O. Kramarov, Ferroelectrics, 18, 249 (1978).

14. K.D. McHenry and B.G. Koepke, unpublished research.

15. G.B. Caso and V.D. Frechette, Bull. Amer. Ceram. Soc., 58, 342 (1979) Abstract Only.

16. K.D. McHenry and B.G. Koepke, Fracture Mechanics of Ceramics, Vol. 5, R.C. Bradt, A.G. Evans, D.P.H. Hasselman and F.F. Lange, ed. Plenum, New York (1983) p. 337.

17. M.J. Cozzolino and G.J. Ewell, IEEE Transactions on Components, Hybrids and Manufacturing Technology, Vol. CHMT-3, 250 (1980).

18. K.D. McHenry and B.G. Koepke, Mat. Res. Soc. Symp. Proc., 72, 113 (1986).

19. J.A. Van Den Avyle and J.J. Mecholsky, Ferroelectrics. 50, 293 (1983).

20. B.G. Koepke and K.D. McHenry, Ferroelectrics, 28, 343 (1980).